Rewiring the altered tryptophan metabolism as a novel therapeutic strategy in inflammatory bowel diseases

Chloé Michaudel, Camille Danne, Allison Agus, Aurélie Magniez, Anne Aucouturier, Madeleine Spatz, Antoine Lefevre, Julien Kirchgesner, Nathalie Rolhion, Yazhou Wang, et al.

OPEN ACCESS

Original research

Rewiring the altered tryptophan metabolism as a novel therapeutic strategy in inflammatory bowel diseases

Chloé Michaudel,[1,2] Camille Danne,[1,2,3] Allison Agus,[1,2] Aurélie Magniez,[1,2] Anne Aucouturier,[1,2] Madeleine Spatz,[1,2] Antoine Lefevre,[4] Julien Kirchgesner ,[2,5] Nathalie Rolhion,[2,3] Yazhou Wang,[1,2] Aonghus Lavelle,[2,3] Chloé Galbert,[2,3] Gregory Da Costa,[1,2] Maxime Poirier,[1,2] Alexia Lapière,[1,2] Julien Planchais,[1,2] Petr Nádvorník,[6] Peter Illes,[6] Cyriane Oeuvray,[2,3] Laura Creusot,[2,3] Marie-Laure Michel,[1,2] Nicolas Benech,[2,3,5] Anne Bourrier,[2,5] Isabelle Nion-Larmurier,[2,5] Cecilia Landman,[2,5] Mathias L Richard,[1,2] Patrick Emond,[4,7] Philippe Seksik,[2,3,5] Laurent Beaugerie,[2,5] Rafael Rose Arguello,[8] David Moulin ,[9] Sridhar Mani,[10] Zdenek Dvorák,[6] Luis G Bermúdez-Humarán,[1,2] Philippe Langella,[1,2] Harry Sokol [1,2,3,5]

► Additional supplemental material is published online only. To view, please visit the journal online (http://dx.doi.org/10.1136/gutjnl-2022-327337).

For numbered affiliations see end of article.

Correspondence to
Professor Harry Sokol, Sorbonne Universite, Paris, Île-de-France, France; harry.sokol@gmail.com

Received 11 March 2022
Accepted 6 October 2022

To cite: Michaudel C, Danne C, Agus A, *et al*. *Gut* Epub ahead of print: [*please include* Day Month Year]. doi:10.1136/gutjnl-2022-327337

ABSTRACT

Objective The extent to which tryptophan (Trp) metabolism alterations explain or influence the outcome of inflammatory bowel diseases (IBDs) is still unclear. However, several Trp metabolism end-products are essential to intestinal homeostasis. Here, we investigated the role of metabolites from the kynurenine pathway.

Design Targeted quantitative metabolomics was performed in two large human IBD cohorts (1069 patients with IBD). Dextran sodium sulphate-induced colitis experiments in mice were used to evaluate effects of identified metabolites. In vitro, ex vivo and in vivo experiments were used to decipher mechanisms involved. Effects on energy metabolism were evaluated by different methods including Single Cell mEtabolism by profiling Translation inHibition.

Results In mice and humans, intestinal inflammation severity negatively correlates with the amount of xanthurenic (XANA) and kynurenic (KYNA) acids. Supplementation with XANA or KYNA decreases colitis severity through effects on intestinal epithelial cells and T cells, involving Aryl hydrocarbon Receptor (AhR) activation and the rewiring of cellular energy metabolism. Furthermore, direct modulation of the endogenous tryptophan metabolism, using the recombinant enzyme aminoadipate aminotransferase (AADAT), responsible for the generation of XANA and KYNA, was protective in rodent colitis models.

Conclusion Our study identified a new mechanism linking Trp metabolism to intestinal inflammation and IBD. Bringing back XANA and KYNA has protective effects involving AhR and the rewiring of the energy metabolism in intestinal epithelial cells and CD4$^+$ T cells. This study paves the way for new therapeutic strategies aiming at pharmacologically correcting its alterations in IBD by manipulating the endogenous metabolic pathway with AADAT.

WHAT IS ALREADY KNOWN ON THIS TOPIC

⇒ Kynurenic acid (KYNA) and xanthurenic acid (XANA) can activate aryl hydrocarbon receptor (AhR)-related genes but their agonist activity is unknown.
⇒ Some tryptophan metabolites are essential for intestinal homeostasis, but activation of IDO pathway can be deleterious.
⇒ AhR activation impacts intestinal epithelial cells proliferation and gut barrier integrity.
⇒ AhR activation impacts T cell differentiation.

WHAT THIS STUDY ADDS

⇒ XANA and KYNA abundance are negatively correlated with intestinal inflammation in mice and humans.
⇒ The kynurenine pathway is composed of protective (KYNA and XANA) and deleterious metabolites (QUIN).
⇒ XANA and KYNA are bona fide AhR ligand.
⇒ XANA and KYNA promote intestinal epithelial cells survival and proliferation through enhancement of mitochondrial respiration.
⇒ XANA and KYNA promote Th17 cells differentiation in a mechanism dependent on glycolysis induction.
⇒ The use of the recombinant aminoadipate aminotransferase (AADAT), to favor KYNA and XANA production, is protective in colitis model.

INTRODUCTION

Inflammatory bowel diseases (IBDs) represent a public health issue in industrialised societies.[1] The precise mechanisms leading to these diseases are linked to an inappropriate immune system response,[2] genetic susceptibilities involving

HOW THIS STUDY MIGHT AFFECT RESEARCH, PRACTICE OR POLICY

⇒ Manipulating the endogenous tryptophan metabolism with AADAT is an attractive new therapeutic strategy in inflammatory bowel disease.

many genes (eg, CARD9, NOD2)[3] and altered intestinal gut microbiota.[4]

In the broad sense, metabolism is the set of chemical reactions in a living organism required for its functioning.[5] The interweaving of metabolism pathways, from amino acid catabolism to glycolysis and mitochondrial respiration, makes it an intricated network crucial for cellular homeostasis,[6] activation or differentiation.[7] Logically, its deregulation is involved in many pathogenesis events.[8 9] Literature has recently pointed out the role of tryptophan (Trp) metabolism in the context of intestinal inflammation.[3 10] Trp can be metabolised following three major pathways: the serotonin and kynurenine (KYNU) pathways (KP), while the indole pathway.[11] The production of indoles by the gut microbiota, which is altered in patients with IBD, is crucial to intestinal homeostasis, notably through their effect on activating the aryl hydrocarbon receptor (AhR).[3 12] The role of serotonin and KP have been highlighted in several chronic inflammatory pathological contexts, from IBD[10 13 14] to metabolic syndrome.[15] The KP is of particular interest as it leads to the production of several end-product metabolites, which have strong biological effects through identified receptors such as AhR (kynurenic acid (KYNA)),[16] GPR35 (KYNA),[17] N-methyl-D-aspartate receptor (KYNA, quinolinic acid (QUIN)).[18] The KP and its host receptor targets are particularly relevant in inflammatory contexts, including IBD, as these conditions are associated with KP activation.[10] Indeed, some KP metabolites impact immune cells functions notably via AhR activation[19] that is involved in the differentiation of T cells,[20] the production of IL-17 and IL-22,[21 22] the maintenance of type 3 innate lymphoid cells (ILC3) in the gut[23] or the antioxidant response.[24] However, the role of many metabolites from the KP in IBD remains poorly defined.

Here, we used targeted quantitative metabolomics to characterise the trp metabolism in colitis models in mice and two large independent human cohorts. We observed a strong negative correlation between the amount of xanthurenic acid (XANA) and KYNA, and intestinal inflammation. Treatment with XANA or KYNA exhibits protective effects in colitis models by modulating the energy metabolism in intestinal epithelial cells (IEC) and T cells. Oxidative phosphorylation is boosted in IEC, leading to an improvement in proliferation and ultimately tissue repair, mediated by the AhR-IL-22 axis. Glycolysis is stimulated in T cells with positive effects regarding activation and polarisation towards T_H17 phenotype. From a therapeutic perspective, we proposed a recombinant enzyme-based strategy to rewire the endogenous Trp metabolism toward the production of XANA and KYNA. We show the efficacy of this strategy in colitis models, thus paving the way for the development of a new class of drugs for IBD.

RESULTS

XANA and KYNA abundance negatively correlates with colitis severity in mice

The KP (figure 1A) is globally considered to play a role in the inflammatory process. To gain insight into the precise role of

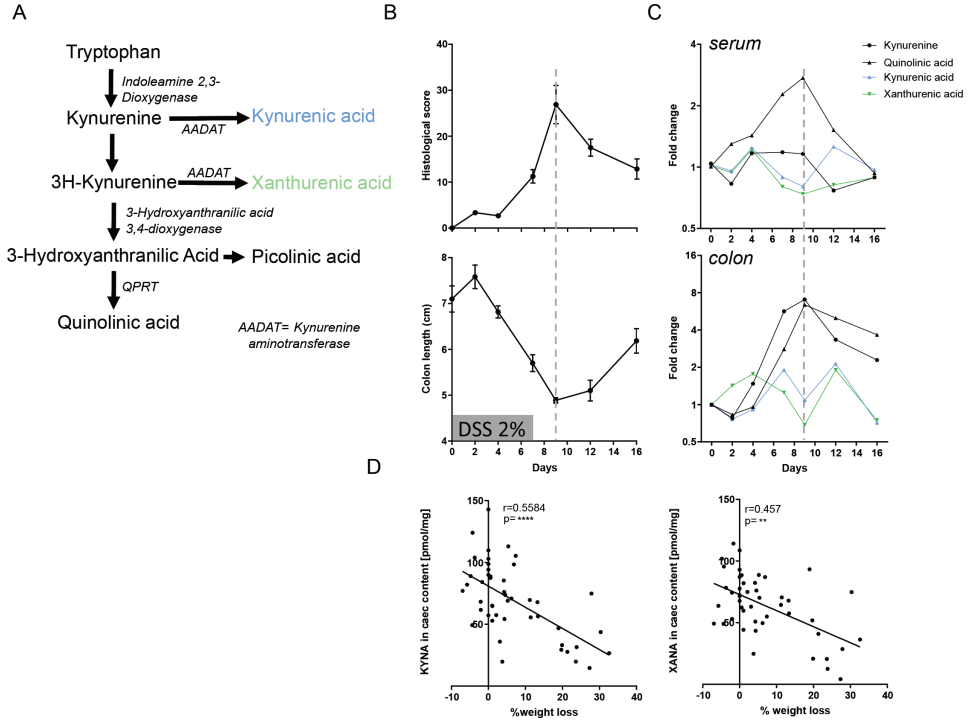

Figure 1 KYNA and XANA abundances are negatively correlated with inflammation during DSS-induced colitis. (A) Kynurenine pathway, (B) histological score and colon length dynamic during the course of DSS-induced colitis, (C) dynamic of kynurenine pathway metabolites in serum and colon tissue during the course of DSS-induced colitis, (D) correlation between KYNA and XANA abundance in the caecum and weight loss. Statistical analysis: n=6–8 per time point, for correlation n=47, Spearman's rank correlation, **: p<0.01, ****: p<0.0001. AADAT, aminoadipate aminotransferase; DSS, dextran sodium sulphate; KYNA, kynurenic acid; XANA, xanthurenic acid.

metabolites downstream of KYNU in intestinal inflammation, we performed a dense time-course experiment in mice submitted to Dextran Sodium Sulphate (DSS)-induced colitis (figure 1B). The peak of inflammation, evaluated by histological scoring and colon length measurement, was observed on day 9. Quantitative targeted metabolomics was used to measure the metabolites of the Indoleamine 2,3-dioxygenase (IDO) pathway in serum and colon. We observed that the dynamics of the metabolites composing this pathway differed from one to another (figure 1C). In particular, the dynamics of KYNU and QUIN positively correlated with inflammation, while the opposite pattern was observed for XANA or KYNA (figure 1C). Similarly, a negative correlation was observed between weight loss and amounts of KYNA and XANA in caecum content (figure 1D), while the opposite was observed with KYNU and QUIN (online supplemental figure S1A,B). These results suggest that specific metabolites of KP, notably KYNA and XANA, could play a protective role in colitis.

XANA and KYNA abundance correlates with disease activity in humans with IBD

We then studied the relevance of these results in a human context. We analysed faecal (n=104) and serum (n=108) samples from 15 patients enrolled in a pilot clinical trial evaluating the effect of faecal microbiota transplantation in Crohn's disease.[25] Quantitative metabolomics analysis targeting Trp metabolites was performed on these samples (online supplemental figure S1C). We observed a negative correlation between several markers of disease activity, including various clinical, endoscopic and biological parameters, with KYNA and XANA (as well as the ratio of KYNA, XANA with their precursors, KYNU and 3-hydroxykynurenine, respectively), while the reverse was noted with KYNU and QUIN (online supplemental figure S1D,E). We then took advantage of a large independent cohort (Suivitheque) of 1069 patients with IBD and 98 healthy subjects (HS) for which serum and faeces (for a subpopulation) were available (online supplemental table S1, figure 2A). Trp metabolites measured in serum by targeted quantitative metabolomics approach significantly discriminated patients with IBD from HS (figure 2B). The differential analysis identified many strongly statistically significant differences between HS and patients with IBD (figure 2C) and also between patients with IBD in flare and in remission (figure 2D). Notably, XANA and KYNA (as well as the ratio of KYNA, XANA with their precursors) were decreased in patients with IBD compared with HS and in patients in flare compared with those in remission (figure 2C–E and online supplemental figure S1F–H). In this second cohort, we also observed a negative correlation between several clinical[26] and biological markers of disease activity and XANA and KYNA (figure 2F). The signal was also confirmed when we correlated the serum concentration of Trp metabolites and several cytokines in a subgroup of 149 patients with IBD, taken randomly in the Suvitheque cohort (the characteristics of these 149 patients are described in online supplemental table S2). Here again, XANA and KYNA negatively correlated with inflammatory cytokines, while the opposite was observed for QUIN (online supplemental figure S1I). A similar signal, although weaker, was observed when looking at metabolites in the stools (online supplemental figure S1J,K). Finally, when considering the subgroup of patients with IBD in remission (n=333), a lower serum level of XANA and KYNA was predictive of a higher risk of occurrence of disease-related clinical events (surgery or flare with the need to initiate a new treatment) (figure 2G).

Taken together, these results in mice and two independent human cohorts show strong negative correlations between the serum and faecal amounts of XANA and KYNA, and intestinal inflammation, and suggest a potential protective role of these metabolites.

Administration of XANA and KYNA protects from DSS-induced colitis

To explore the potential protective role of XANA and KYNA in intestinal inflammation settings, mice submitted to DSS-induced colitis were orally gavaged with XANA or KYNA (online supplemental figure S2A), leading to an elevation in the serum levels of these metabolites (online supplemental figure S2B). As demonstrated by the reduction in weight loss (figure 3A), disease activity index (figure 3B), colon length shortening (figure 3C) and histological score (figure 3D,E), treatment with XANA and KYNA induced a strong protective effect compared with the control group. Interestingly QUIN, whose abundance was positively correlated with inflammation severity, exhibited proinflammatory effects (online supplemental figure S2C–E). The protective effect of XANA and KYNA was confirmed by colonic transcriptomic response at day 12 with the downregulation of many pro-inflammatory cytokines and chemokines genes (eg, IL-6, CXCR1, figure 3F) in mice treated with these metabolites. The same protective effect was observed when XANA and KYNA were administered through intraperitoneal injection (online supplemental figure S2F–J).

Altogether, these results demonstrate a protective effect of XANA and KYNA in a colitis model in mice.

XANA and KYNA act on viability and proliferation of IECs through AhR activation and IL-22

To investigate the mechanism of the protective effects of XANA and KYNA in colitis, we started by exploring a potential effect on IEC. As shown by the increased staining for Ki67 in the recovery phase at day 12 in colitis experiment, XANA and KYNA stimulated the proliferation of IEC and intestinal healing compared with control mice (figure 4A). In addition, a wound healing assay, carried out with human IEC, showed that XANA and KYNA stimulate cell proliferation and, therefore, faster wound repair (figure 4B,C). KYNA has been shown to activate GPR35[17] and the AhR pathway.[16] While the protective effects of XANA and KYNA were maintained in GPR35$^{-/-}$ mice (online supplemental figure S3A,B), it was lost in AhR$^{-/-}$ mice (figure 4D, online supplemental figure S4A,B). Indeed the activation of AhR by XANA and KYNA was seen in vivo, as demonstrated by the induction of the expression of Cyp1a1, a major AhR target gene, in the colon of mice treated with XANA or KYNA for 12 days (figure 4E). FICZ (6-formylindolo(3,2b) carbazole), an AhR agonist, recapitulated the effect of KYNA and XANA (figure 4B,C). Moreover, the healing effect of XANA and KYNA in wound healing assay was lost in the presence of the AhR inhibitor CH223191 (figure 4F,G), suggesting that AhR, which is known to stimulate IEC proliferation,[27 28] is at least partly involved in the underlying mechanisms. Experiments with a reporter cell line confirmed that both XANA and KYNA activate the AhR pathway (figure 4H). Similar results were obtained with human IEC cell lines in which the two metabolites induced the nuclear translocation of AhR (online supplemental figure S4C) and the expression of the AhR target gene Cyp1a1 (online supplemental figure S4D). Finally, the radioligand displacement assay showed that XANA and KYNA were effective in displacing radiolabeled TCDD (2,3,7,8-tetrachlorodibenzo-p-dioxin),

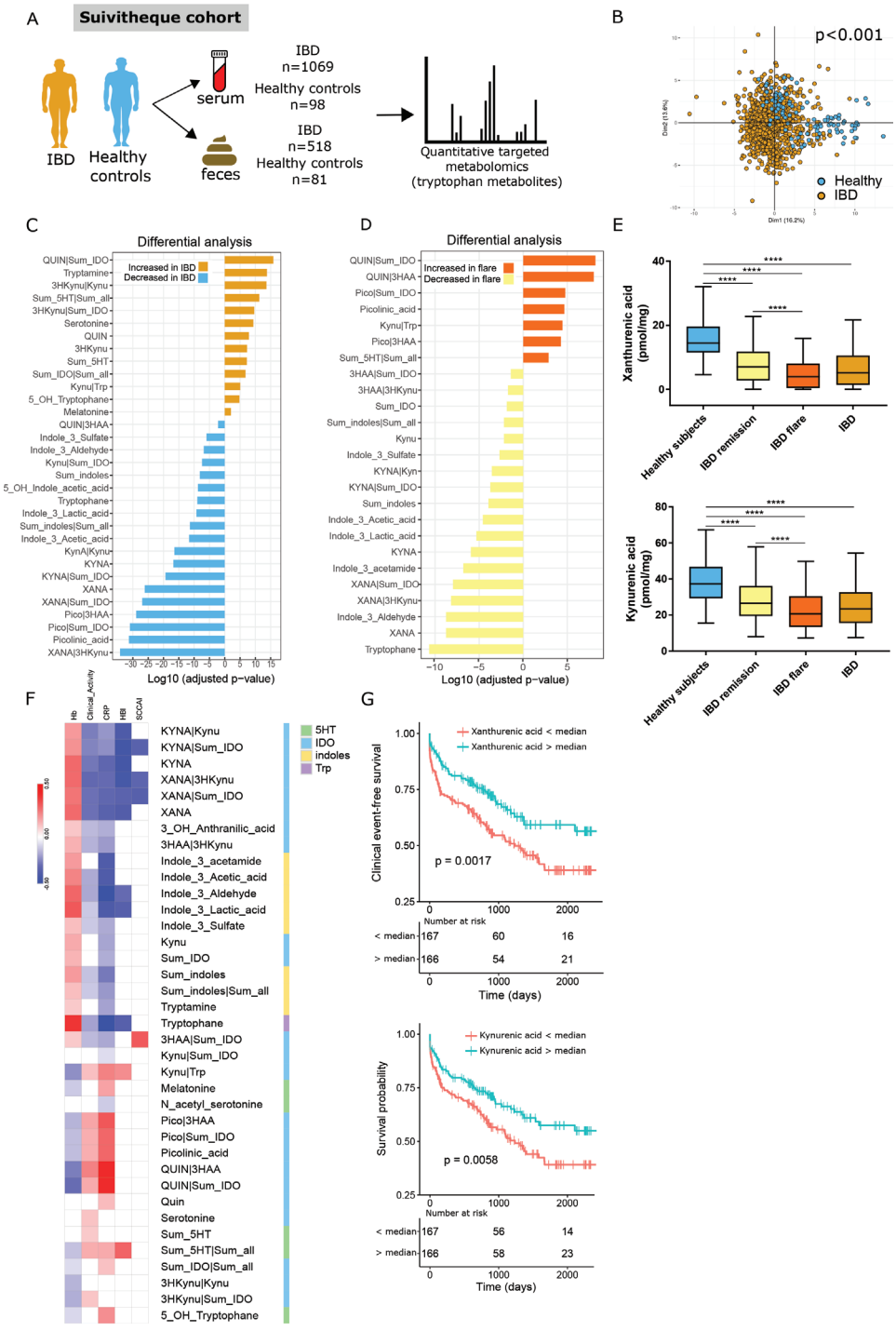

Figure 2 KYNA and XANA abundances correlate with disease activity in humans with IBD: Suivitheque cohort. (A) Design of the Suivitheque cohort. (B) PCA analysis based on trp metabolites in serum. (C) Differential analysis of the abundance of TRP metabolites in serum between patients with IBD versus HS (adjusted p value bH). (D) differential analysis of the abundance of TRP metabolites in serum between patients with IBD in flare versus remission (adjusted p value bH). (E) XANA and KYNA amount in serum (ANOVA with correction for FDR bH). (F) Correlation between the amount of tryptophan metabolites in serum and disease activity parameters. Spearman, p<0.05, q<0.1 (BH). (G) Clinical event-free survival according to XANA and KYNA levels in serum. Only patients in remission were included in this analysis. Two groups were defined according to the median level of XANA and KYNA. Statistical comparison was performed with a log-rank test. ANOVA, analysis of variance, ****: p<0.0001; CRP, C reactive protein; FDR, false discovery rate; Hb, haemoglobin; HBI, Harvey-Bradshaw Index; HS, healthy subjects; IBD, inflammatory bowel disease; IDO, indoleamine 2,3-dioxygenase; KYNA, kynurenic acid; PCA, principal component analysis; SCCAI, Simple Clinical Colitis Activity Index; XANA, xanthurenic acid.

a high-affinity AhR ligand, with a stronger effect for XANA (figure 4I). The radiodisplacement of a ligand with high affinity for AhR (TCDD), provides evidence that XANA and KYNA are true ligands for AhR.

Interestingly, XANA and KYNA still exhibited some level of protection in $AhR^{\Delta IEC}$ mice that are deficient for AhR only in IECs (figure 4J–L), suggesting that other cell types are also involved in the mechanisms of action. In the gut, besides the

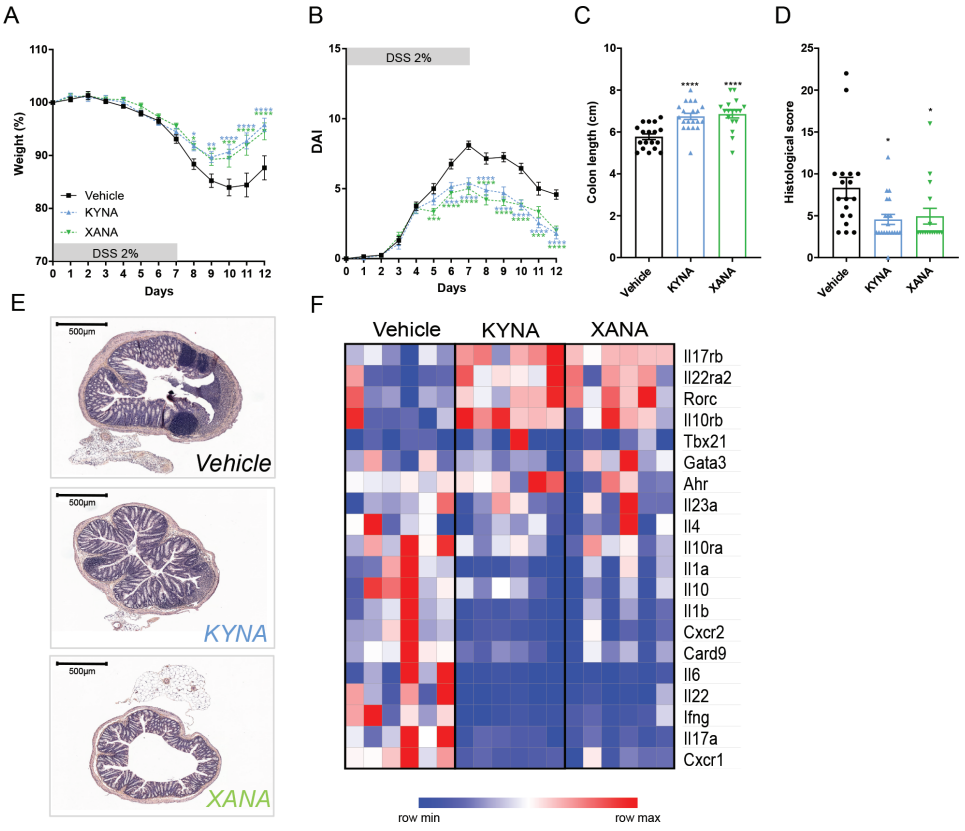

Figure 3 IDO metabolites, XANA and KYNA protect against DSS-induced colitis. (A) Body weight loss, (B) DAI, (C) colon length, (D) histological score, (E) colon histology pictures and (F) nanostring colon transcriptomic results at day 12. Each column represents a mouse. Statistical analysis: n=16–20 mice per group, two-way or one-way ANOVA, with Bonferroni post test, *: p<0.05, **: p<0.01, ***: p<0.001, ****: p<0.0001. ANOVA, analysis of variance; DAI, disease activity index; DSS, dextran sodium sulphate; IDO, indoleamine 2,3-dioxygenase; KYNA, kynurenic acid; XANA, xanthurenic acid.

direct activation of epithelial cells, AhR agonists also stimulate lymphoid cells to produce IL-22, which has a protective effect in colitis settings, notably by inducing the production of antimicrobial peptides, such as RegIIIγ and RegIIIδ, by IEC.[11] Interestingly, the expression of Il-22, RegIIIγ and RegIIIδ was upregulated (statistically significant for IL-22 only) in the colon of mice treated by XANA and KYNA (online supplemental figure S4E). The protective effect of XANA and KYNA was decreased in IL-22$^{-/-}$ mice (online supplemental figure S4F,G), suggesting that the induction of IL-22 is involved in the mechanism underlying the effects of XANA and KYNA.

Taken together, these results demonstrate that XANA and KYNA are bona fide AhR ligands. Their protective effects are at least partly mediated by direct activation of the AhR pathway, as well as indirect effect through AhR-IL-22 axis activation. IEC are involved in the mechanisms of action of KYNA and XANA, together with other cell types.

XANA and KYNA act on mitochondrial metabolism in epithelial cells

IEC functions rely on energy and particularly on mitochondrial activity. In the colon, the dominant source of energy for epithelial cells is the short-chain fatty acid (SCFA) butyrate, which is produced from the digestion of fibres by the gut microbiota. Butyrate enters epithelial cells through specific transporters and diffuses into the mitochondria, where it undergoes β-oxidation, leading to the production of acetyl-CoA, NADH and FADH2 that feed the TCA cycle and the electron transport chain to produce ATP. The luminal content of mice treated by XANA or KYNA for 12 days showed a drop in the concentration of SCFA compared with untreated controls (figure 5A). The analysis of the gut microbiota composition by next-generation sequencing did not indicate any significant effect of KYNA and XANA after 12 days of gavage (online supplemental figure S5A–D). This suggests that the decreased SCFA concentration may be due to an increase in consumption by host cells rather than a decrease in production by the gut microbiota. The increased expression of two SCFA transporters, Smct and Mct-1, in the colon of mice treated with XANA or KYNA (figure 5B), as well as the increased consumption of butyrate by IEC treated with XANA or KYNA (online supplemental figure S5E), support this hypothesis. We then explored the effect of XANA and KYNA on the energy metabolism of human IEC. The proportion of cells with dysfunctional mitochondria (in connection with an altered energy metabolism), defined by a positive Mitotracker Green staining with a negative Mitotracker Red staining, was decreased after treatment with XANA or KYNA (figure 5C). Interestingly, even mitochondria classified as dysfunctional were in better shape in XANA or KYNA-treated cells, as shown by a higher Mitotracker Red MFI than in control cells (figure 5D). Beyond a smaller proportion of dysfunctional mitochondria, XANA and KYNA-treated cells exhibited a higher respiratory activity (figure 5E) and greater maximal respiration (figure 5F,G), while the glycolysis was not impacted (figure 5H,I). The same effect was recapitulated on colon epithelial cells isolated from mice gavaged with KYNA and XANA for 12 days (figure 5J), and in colon organoids treated

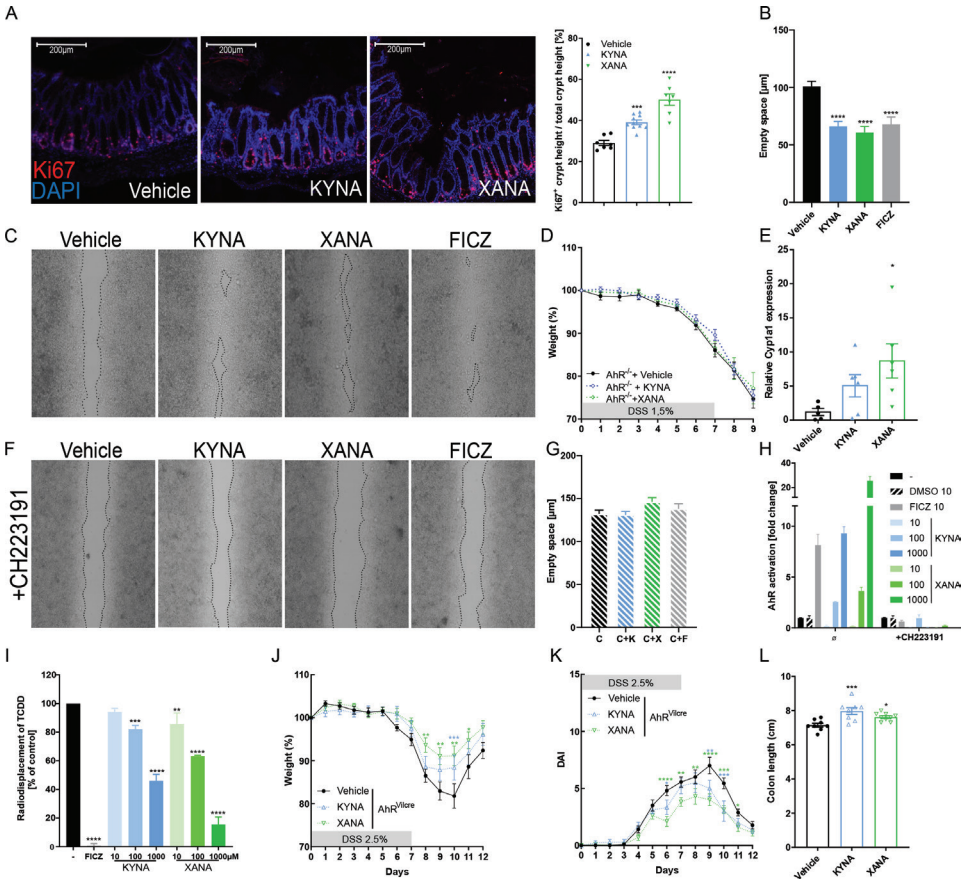

Figure 4 KYNA and XANA promote intestinal epithelial cells viability and proliferation through AhR. (A) Ki67 and DAPI staining in mouse colon at day 12 of a DSS model and quantification. (B, C) Scratch test on HT-29 cells treated with KYNA, XANA or FICZ: representative pictures and quantification of empty space. (D) Colitis protection by KYNA and XANA is abrogated in $AhR^{-/-}$ mice. (E) Oral gavage of KYNA and XANA for 12 days activate the expression of the AhR target gene, CYP1A1 in the colon. (F, G) Scratch test on HT-29 cells treated with KYNA, XANA, FICZ, with the AhR antagonist CH223191. (H) AhR reporter cell line activation and (I) radio displacement of TCDD induced by KYNA and XANA. (J–L) colitis protection by KYNA and XANA are partly conserved in $AhR^{\Delta IEC}$ mice. Data represent one out of two independent experiments. Statistical analysis: for scratch test 100 measures per slide, in vitro experiment n=3 and for in vivo and ex vivo experiment n=5–10 mice per group, two-way or one-way ANOVA, with Bonferroni post test, *: p<0.05, **: p<0.01, ***: p<0.001, ****: p<0.0001. AhR, aryl hydrocarbon receptor; ANOVA, analysis of variance;DSS, dextran sodium sulphate; KYNA, kynurenic acid; XANA, xanthurenic acid.

with KYNA and XANA (figure 5K). The positive effect of XANA and KYNA on tissue repair disappeared when mitochondrial respiration was inhibited with oligomycin (Oligo) (figure 5L,M). Furthermore, cell proliferation increased in mouse colon organoids treated with KYNA or XANA (figure 5N). This effect was abrogated by oligomycin. Therefore, by promoting mitochondrial respiration, the effects of XANA and KYNA on epithelial cells' energy metabolism contribute to tissue integrity and could, at least partly, explain their protective effects in colitis settings.

XANA and KYNA effects are dependent on adaptative immunity and particularly T_H17 cells

As the above-described results suggest that IEC are not the only cell types involved in the mechanisms of action of XANA and KYNA, we explored the potential role of other cells.

The expression of several chemokines (ie, Ccl22, Ccl20) involved in T cells recruitment and T-cell-related transcription factor (ie, Nfatc2, Nfactc3) were induced in the colon of XANA or KYNA-treated mice (figure 6A). We reasoned that T cells, which are crucial actors in colitis and IBD, might be involved in the therapeutic effects of XANA or KYNA. In $Rag2^{-/-}$ mice, which have no functional T and B cells, the effect of XANA and KYNA was lost (figure 6B,C, online supplemental figure S6A–H), showing that adaptive immunity is involved in the protection induced by the two metabolites. In vivo, after 7 days of DSS exposure, XANA and KYNA-treated wild-type (WT) mice exhibited an increased abundance of T_H17 and $Ror\gamma t^+$ T cells, but not T_H1 cells (online supplemental figure S6I,J). In vitro, XANA and KYNA promoted T cell differentiation towards T_H17 (figure 6D and online supplemental figure S6K).

Taken together, these results show that adaptive immunity is involved in the protective effects of XANA and KYNA, with a particular role for T_H17 cells.

XANA and KYNA stimulate glycolysis in lymphocytes through AhR

Energy metabolism has a strong impact on T cells functions.[29] As XANA and KYNA impact energy metabolism in IEC, we hypothesised it could also be the case with T cells. In Jurkat human T cell line and mouse primary $CD4^+$ T cells, XANA and KYNA induced a reduction in mitochondrial metabolism as demonstrated by the decreased Mitotracker Red fluorescence (figure 6E,F). This result

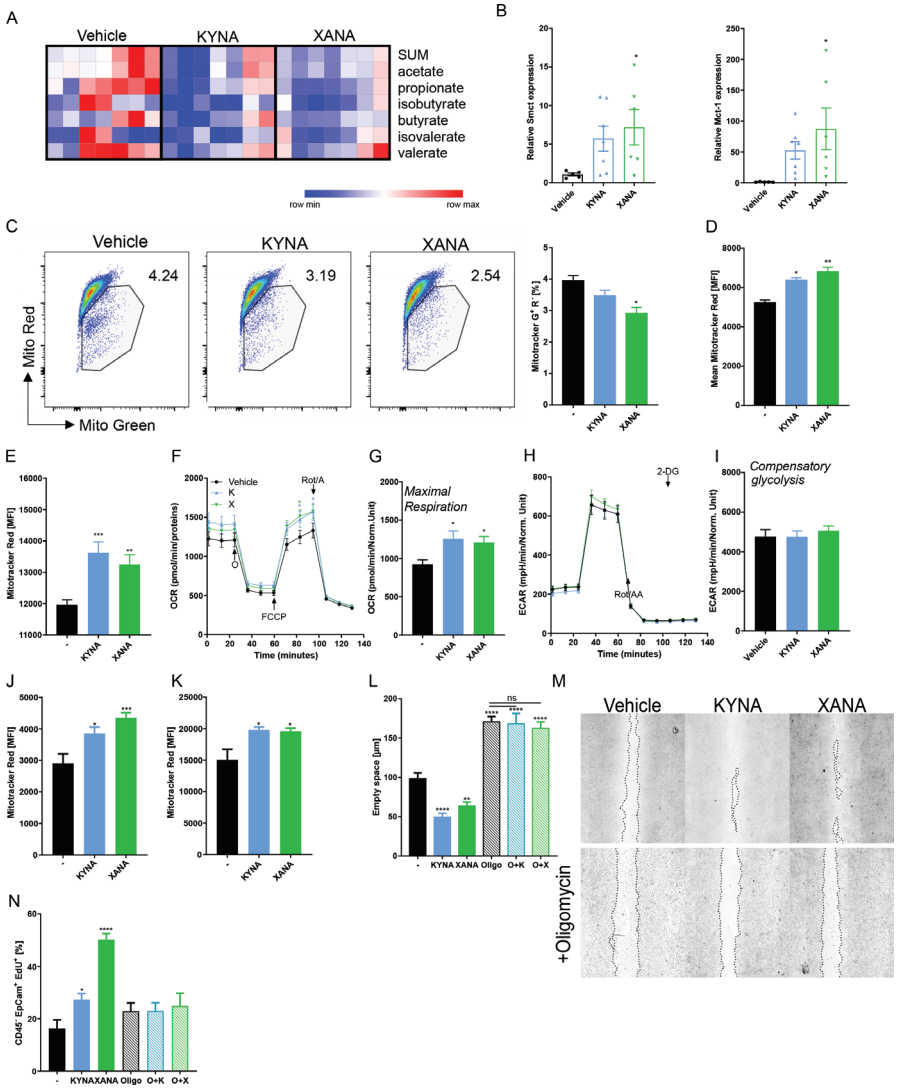

Figure 5 KYNA and XANA improved mitochondrial metabolism in epithelial intestinal cells. (A) SCFA dosages in cecum content and (B) relative SMCT and MCT-1 expression in murine colon at steady state in mouse after 12 days of KYNA and XANA gavage. (C) Dysfunctional mitochondria (MitoRed$^-$ and MitoGreen$^+$) in HT-29 cells after 72 hours of KYNA or XANA stimulation (100 µM). (D) MitoRed MFI in dysfunctional mitochondria (MitoRed$^-$ MitoGreen$^+$) from HT-29 cells. (E) MitoRed MFI in MitoRed$^+$ HT-29 population. (F) Mitochondrial metabolisms with ocr measurements and (G) maximal respiration in Seahorse assay on HT-29 cells after 72 hours of KYNA or XANA stimulation. (H) Glycolysis metabolism, with ECAR measurements and (I) compensatory glycolysis in Seahorse assay on HT-29 cells after 72 hours of KYNA or XANA stimulation. (J) MitoRed MFI of CD45$^-$EpCAM$^+$ cells from the colon of mice gavaged for 12 days with KYNA or XANA. (K) MitoRed MFI of CD45$^-$EpCAM$^+$ cells from mice colon organoids 72 hours after KYNA, XANA and oligomycin treatment (5 µM). (L, M) Scratch test on HT-29 cells treated with KYNA, XANA in presence of oligomycin (5 µM): representative pictures and quantification of empty space. (N) Proliferation assay with EdU on mouse colon organoids 72 hours after KYNA, XANA and oligomycin treatment (5 µM). Data represent one out of two independent experiments. Statistical analysis: for in vitro experiment n=3–6 and for in vivo experiment n=5–7 mice per group, two-way or one-way ANOVA, with Bonferroni post test, *: p<0.05, **: p<0.01, ***: p<0.001, ****: p<0.0001. ANOVA, analysis of variance; EdU, 5-éthynyl-2′-déoxyuridine; KYNA, kynurenic acid; MFI, mean fluorescence intensity; SCFA, short-chain fatty acid; XANA, xanthurenic acid.

was confirmed by Seahorse assay that showed a reduction of maximal respiration (figure 6G). However, the proportion of dysfunctional mitochondria was unchanged (online supplemental figure S6L). This effect was AhR-dependent as it was recapitulated by AhR agonist (figure 6F) and lost in AhR deficient CD4$^+$ T cells (figure 6H). Seahorse assay also showed that treatment with XANA or KYNA stimulates glycolysis in T cells, as demonstrated by the increased extracellular acidification rate (ECAR) at basal state (basal glycolysis) and after blocking mitochondrial respiration with rotenone and antimycin A (compensatory glycolysis) (figure 6I). To evaluate in vivo the effects of XANA and KYNA on T cells energy metabolism, we used a newly developed assay, SCENITH (Single Cell mEtabolism by profiling Translation inHibition).[30] This method is based on quantifying metabolism-dependent translation rates through puromycin incorporation into nascent proteins. The use of specific inhibitors allows the estimation of glucose dependence, mitochondrial dependence, glycolytic capacity, fatty acid (FAO) and amino acid oxidation (AAO) capacity. Metabolic profile of T cells from the mesenteric lymph nodes of KYNA-treated and XANA-treated mice during DSS-induced colitis confirmed a decrease in mitochondria dependence and an increase in glycolytic capacity, with no change in

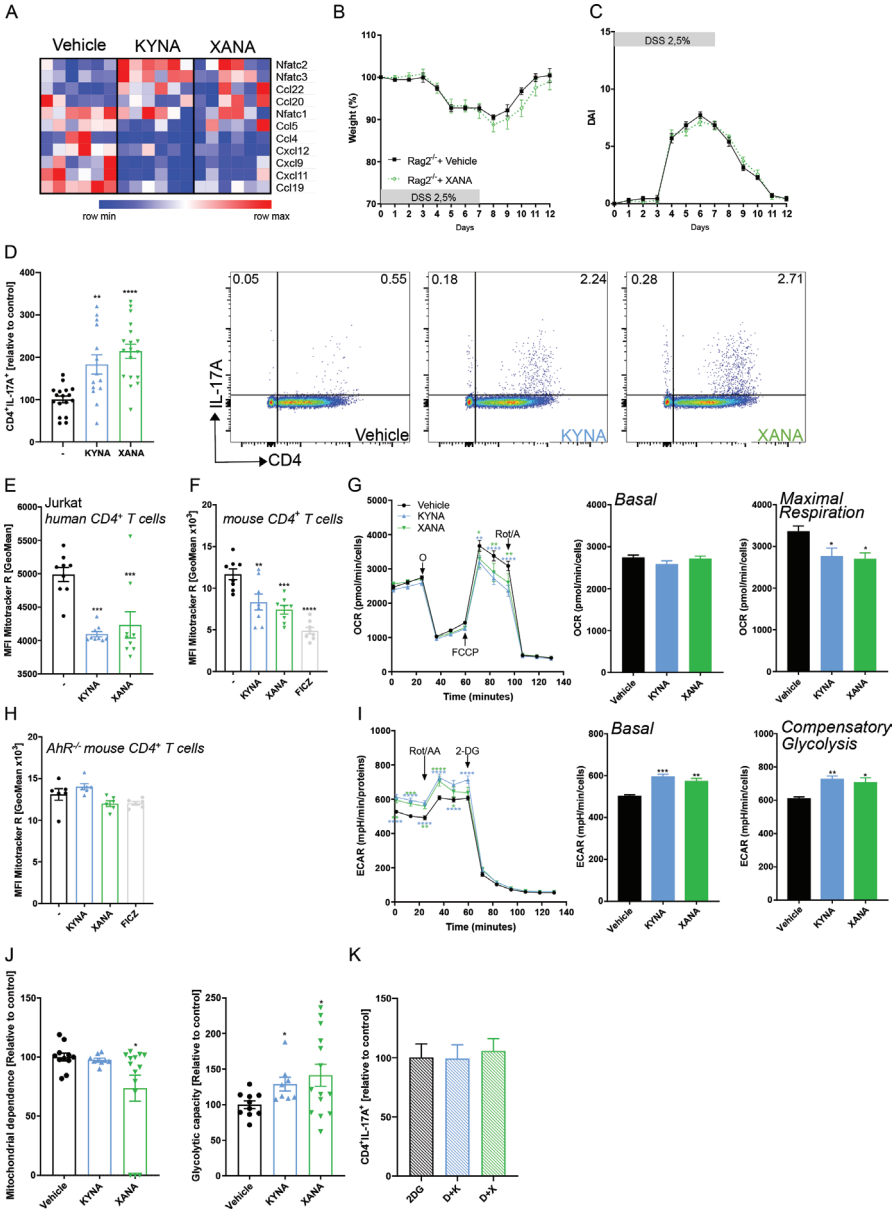

Figure 6 Adaptative immunity is involved in KYNA and XANA protective effects. (A) Lymphocytes-related genes colonic expression after 12 days of oral gavage with KYNA or XANA. (B) Body weight loss, (C) DAI in Rag2$^{-/-}$ after XANA administration. (D) Action of KYNA and XANA on T_H17 cell differentiation in vitro. (E) Mitotracker red MFI in Jurkat cells and (F) mouse CD4$^+$ T cells after a stimulation with KYNA and XANA. (G) Mitochondrial metabolisms with OCR measurements, basal and maximal respiration in Seahorse assay on Jurkat cells after KYNA or XANA stimulation for 72 hours. (H) Mitotracker red MFI in AhR$^{-/-}$ mouse CD4$^+$ T cells. (I) Glycolysis metabolism, with ECAR measurements, basal and compensatory glycolysis. (J) Mitochondrial dependence and glycolytic capacity of mouse MLN CD4+T cells assessed by SCENITH at day 9 of DSS-induced colitis. (K) 2DG action on T_H17 differentiation in the presence of KYNA and XANA. Data represent one out of two independent experiments. Statistical analysis: for in vitro experiment n=6–9, ex vivo experiments n=10–14 and for in vivo experiment n=7 mice per group, t-test or two-way or one-way ANOVA, with Bonferroni post-test, *: p<0.05, **: p<0.01, ***: p<0.001, ****: p<0.0001. ANOVA, analysis of variance; DSS, dextran sodium sulphate; KYNA, kynurenic acid; MFI, mean fluorescence intensity; SCENITH, Single Cell mEtabolism by profiling Translation inHibition; XANA, xanthurenic acid.

FAO and AAO capacity (figure 6J and online supplemental figure S6M,N). In addition, blocking glycolysis with 2DG inhibited the XANA and KYNA-induced T_H17 differentiation (figure 6K and online supplemental figure S6K). These results demonstrate that the T_H17 polarisation induced by XANA and KYNA is mediated by the modulation of cellular energy metabolism towards glycolysis. This effect is AhR-dependant and contributes to the protective effect of XANA and KYNA.

Modulation of endogenous TRP metabolism towards XANA and KYNA using recombinant aminoadipate aminotransferase protects from DSS-induced colitis

From a therapeutic perspective, we speculated that diverting the endogenous Trp metabolism by favouring the production of anti-inflammatory metabolites while decreasing the production of potential proinflammatory ones might be an attractive strategy. Kynurenine aminotransferase 2, also called AADAT (aminoadipate aminotransferase), is the common enzyme that catalyses the

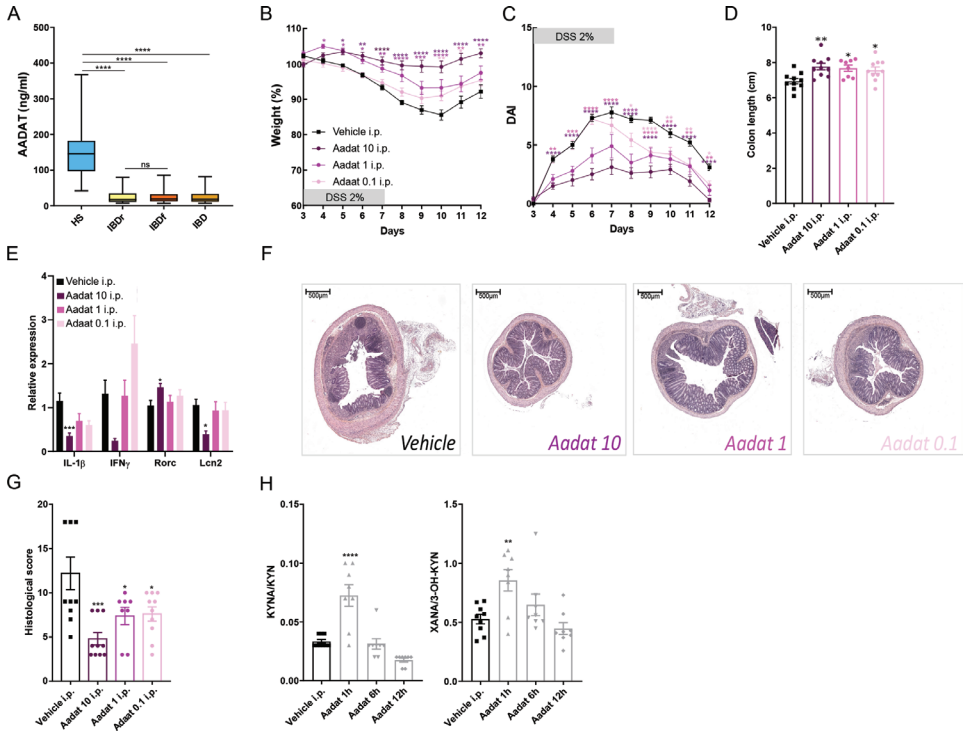

Figure 7 AADAT administration protects from DSS-induced colitis. (A) AADAT quantified in serum of healthy subjects (HS, n=39) and patients with IBD in remission (R, n=238) or in flare (F, n=248), (B) body weight loss, (C) DAI, (D) colon length, (E) relative genes expression of IL-1β, IFNγ, RORc and LCN2, (F) colon histology pictures and (G) histological score. (H) Serum metabolite levels in mice at day 9 of DSS-induced colitis, 1, 6 and 12 hours after AADAT injection. Statistical analysis: n=8–10 mice per group, two-way or one-way ANOVA with Bonferroni post-test, *: p<0.05, **: p<0.01, ***: p<0.001, ****: p<0.0001. AADAT, aminoadipate aminotransferase; ANOVA, analysis of variance; DAI, disease activity index; DSS, dextran sodium sulphate; IBD, inflammatory bowel disease; ns, not significant.

transformation of kynurenine and 3H-kynurenine into KYNA and XANA, respectively (figure 1A). Moreover, its abundance is dramatically reduced in the serum of human patients with IBD (figure 7A and online supplemental figure S7A). In order to evaluate the therapeutic potential of AADAT in intestinal inflammation, we first expressed murine AADAT in *Escherichia coli* and purified it using affinity chromatography. The functionality of the newly generated enzyme was confirmed in vitro by showing the consumption of kynurenine and 3H-kynurenine and the production of XANA and KYNA (online supplemental figure S7B–H). Three different doses of AADAT were then administered intraperitoneally to mice submitted to DSS-induced colitis. AADAT administration induced a strong dose-response protective effect, as demonstrated by the improved weight loss, DAI, colon length and histological score (figure 7B–G). The KYNA/KYN and XANA/3OH-KYN ratio significantly increased in serum on day 9, 1 hour after AADAT injection, clearly showing the functional effect on the targeted metabolism pathway (figure 7H).

In summary, these last results show that recombinant AADAT delivery has an attractive therapeutic potential in IBD, through the modulation of the endogenous Trp metabolism.

DISCUSSION

The incidence of IBD is growing everywhere in the world, representing a global pandemic. To better understand the disease and develop new therapeutic options, several actors involved in the pathogenesis are actively investigated, including the immune system and the gut microbiota. Metabolism emerged as a new player in immune functions and inflammation with the advent of the new field of immunometabolism.[29] However, the role of specific metabolites and their mode of action remain mostly elusive. Here, we deliberately focused on Trp metabolism, which has been recognised as a crucial actor in intestinal homeostasis through the generation of active end-products both by host cells and the gut microbiota.[11] Using targeted quantitative metabolomics on samples from a dense time-course experiment in mice and two large human datasets, we identified XANA and KYNA as candidate anti-inflammatory metabolites. We showed that XANA and KYNA exhibit anti-inflammatory effects through action on IEC and T cells. This protective effect was at least partly AhR-dependent and mediated by the modulation of cellular energy metabolism. By administrating the recombinant AADAT enzyme, we were able to hijack the endogenous Trp metabolism toward the production of XANA and KYNA and protect mice from colitis.

Although Trp metabolism was previously explored in IBD,[10 11] the current study, encompassing the analysis of samples from a randomised controlled trial evaluating FMT in CD, and from a large cohort of 1069 patients with IBD, is the greatest effort with this aim to date. In order to generate FAIR data, we used a sensitive, easily reproducible and validated technology for the absolute quantification of all tryptophan metabolites by LC-MS/MS (Liquid Chromatography coupled to tandem Mass Spectrometry), which can be used for the exploration of a large number of samples.[31] We identified XANA and KYNA as negatively correlated with several clinical, biological and endoscopic markers of disease activity, as well as with several proinflammatory cytokines. Moreover, lower levels of XANA and KYNA were predictive of relapse in patients with IBD in remission, supporting a potentially active role in the inflammatory process.

In colitis models in mice, we confirmed the anti-inflammatory effects of XANA and KYNA and demonstrated their effects on IEC and T cells. XANA and KYNA promoted IEC proliferation, supporting tissue integrity and healing processes. The two protective metabolites impacted T cells phenotype, notably by promoting T_H17 differentiation. Depending on the context, stimulation of the T_H17 axis can have detrimental or protective effects.[32] Indeed, IL-17A promotes the integrity of the epithelial barrier by inducing claudin expression and thus reinforcing tight junctions in IEC.[33] It is also involved in mounting the appropriate response towards bacteria and fungi, a crucial function at the host–microbiota interface in the gut.[21 34] This protective effect of IL-17 has been pointed out in humans, as blocking IL-17 in patients with Crohn's disease exacerbates intestinal inflammation,[35] and it can promote intestinal inflammation in patients with psoriasis or spondyloarthritis. The precise contributions of IEC and T cells in the therapeutic effects of XANA and KYNA could not be determined. However, T cells seem to predominate as effect of XANA and KYNA was completely lost in $Rag2^{-/-}$ mice while it was only partially lost in $AhR^{\Delta IEC}$ mice.

KYNA is a known agonist for GPR35, an IBD susceptibility gene.[36] However, its protective effect and the one of XANA were not dominantly mediated by this receptor as it was still observed in $GPR35^{-/-}$ mice. On the other hand, AhR activation was largely involved. KYNA was previously shown to be able to activate AhR.[37] We confirmed this result and demonstrated that XANA, together with KYNA, are bona fide AhR agonists. The protective effect on IEC and T cells was at least partly linked to a modulation of cellular energy metabolism. In IEC, mitochondrial activity, which is the dominant energy source in colonocytes,[29 38] was boosted and promoted cellular proliferation and intestinal barrier restoration. In T cells, XANA and KYNA induced an energy switch towards glycolysis, the favourite energy source of activated effector T cells.[29 39] These effects on energy metabolisms were involved in the protective effects of XANA and KYNA. Interestingly, AADAT, the enzyme producing both XANA and KYNA, is a mitochondrial protein. Along with the transformation of KYNU and 3-H kynurenine into KYNA and XANA, AADAT transform 2-oxoglutarate, a TCA cycle intermediate, into glutamate according to the following reactions: KYNU+2-oxoglutarate<=>KYNA+ glutamate+ H_2O and 3-H kynurenine+2-oxoglutarate<=>XANA+glutamate+ H_2O. This is consistent with the impact of manipulating this metabolic pathway on cellular energy metabolism.

In IBD, the current treatment options are based on immunosuppressants that can induce significant side effects, including an increased risk of neoplasias and infections. In this setting, the concepts and therapeutic targets are relatively archaic. As a final step, we evaluated a new therapeutic strategy aiming at engineering the endogenous Trp metabolism to promote the production of XANA and KYNA. The exogenous administration of a recombinant version of AADAT was successfully protecting mice from colitis. In contrast to most of the therapeutic strategies that aim at blocking a proinflammatory agent or pathway, this approach aims at restoring the normal production of anti-inflammatory metabolites while decreasing at the same time the production of proinflammatory ones, such as quinolinic acid.

In summary, our study identified a new mechanism linking Trp metabolism to intestinal inflammation and IBD. The skewed metabolism in the overactivated kynurenine pathway is associated with a relative deficiency in the anti-inflammatory metabolites XANA and KYNA. Bringing back these metabolites has protective effects involving AhR and the rewiring of the energy metabolism in IEC and CD4+T cells. In addition to providing key evidence of the importance of Trp metabolism in the maintenance of intestinal homeostasis, this study paves the way for new therapeutic strategies aiming at pharmacologically correcting its alterations in IBD by manipulating the endogenous metabolic pathway with AADAT.

MATERIAL AND METHODS

see online supplemental material and methods section.

Mouse model

All gene-deficient and WT mice were on the C57BL/6 background. All mice used were female, between 7 and 10 weeks old. Animal experiments were performed according to local ethical panel and the Ministère de l'Education Nationale, de l'Enseignement Supérieur et de la Recherche, France under agreement Apafis 19750-2019041014309428.

IBD cohorts

The population from the IMPACT clinical trial that evaluated the effect of FMT in CD (NCT02097797) was described elsewhere.[25]

KP metabolites

KYNA and XANA were administered daily by oral gavage (400 mg/kg and 300 mg/kg, respectively, Sigma) or by intraperitoneal injection (5 mg/kg and 4 mg/kg, respectively).[40] For in vitro experiments, KYNA and XANA were used at a concentration of 10–1000µM.

Seahorse

HT-29 (10 000 cells per well, plated 72 hours before the experiment) or Jurkat cells (200 000 cells per well, plated in poly-L-lysine precoated plate immediately before the experiment) were incubated with KYNA (100 µM), XANA (100 µM) or FICZ (0.2 ng/mL) for 72 hours. The experiments were performed according to manufacturer instructions.

DSS-induced colitis model

To induce colitis, mice were administered drinking water supplemented with dextran sulfate sodium (DSS; MP Biomedicals, LLC, Aurora, Ohio, USA) for 7 days and were then allowed to recover by drinking unsupplemented water for the next 5 days. Different percentages of DSS were used in the experiments, depending on the product batch and the mice genotype, to avoid a too high mortality rate.

Nanostring

RNA was extracted from the colon with RNeasy Mini Kit (Qiagen) and controlled with a bioanalyser (Agilent 2100 Bioanalyzer System) with RNA Nano protocol's instructions. XT_PGX_MmV1 Immunology kit was used following manufacturer's instructions.

Mitotracker assay

MitoTracker Green FM (1/1500) and MitoTracker Deep Red (1/1000) were added in FACS buffer for 15 min at RT (ThermoFisher Scientific) before analysis.

Single Cell mEtabolism by profiling translation inHibition

SCENITH assay was performed as previously described.[30]

Scratch test
IBIDI technology was used to realise perfect wounds on HT-29 cells' layers. Stimulation was performed with KYNA (100 µM), XANA (100 µM) and FICZ (0.2 pg/µL) with or without CH223191 (Sigma, 10 µM), for 72 hours.

Lamina propria immune cells preparation
As previously described, colonic lamina propria cells preparation was performed.[41]

qPCR analysis
According to the manufacturer's instructions, total RNA was isolated from colon samples or cell suspensions using an RNeasy Mini Kit (Qiagen) Quantitative RT-PCR was performed using QuantiTect Reverse Transcription Kit (Qiagen) and then a Takyon SYBR Green PCR kit (Eurogentec) or Luna Universal One-Step RT-qPCR Kit (New England Biolabs) in a StepOnePlus apparatus (Applied Biosystems) with specific mouse oligonucleotides.

Histology
The histological score, on H&E staining slides, was described previously.[42] Immunofluorescence staining was performed according to standard staining methods on a Leica BOND RX.

SCFA dosage
SCFA dosage was performed as previously described.[41]

Targeted quantitative metabolomics
The method has been described previously.[43]

AADAT in human samples
AADAT was quantified by ELISA following manufacturer's instruction (XpressBio, XPEH1430).

Radio-ligand binding assay
Ligand binding to the cytosolic proteins was determined by the hydroxyapatite binding protocol and scintillation counting as described elsewhere.[44]

Author affiliations
[1]Université Paris-Saclay, INRAe, AgroParisTech, Micalis institute, Jouy-en-Josas, France
[2]Paris Center for Microbiome Medicine (PaCeMM) FHU, Paris, France
[3]Sorbonne Université, INSERM UMRS-938, Centre de Recherche Saint-Antoine, CRSA, AP-HP, Paris, France
[4]UMR 1253, iBrain, University of Tours, Inserm, 37044 Tours, France
[5]Gastroenterology department, Saint Antoine Hospital, APHP, Paris, France
[6]Department of Cell Biology and Genetics, Faculty of Science, Palacky University, Olomouc, Czech Republic
[7]CHRU Tours, Medical Biology Center, Tours, France
[8]Aix Marseille Univ, CNRS, INSERM, CIML, Centre d'Immunologie de Marseille-Luminy, Marseille, France
[9]CNRS, IMoPA, Université de Lorraine, Vandoeuvre-lès-Nancy, France
[10]Molecular Pharmacology, Genetics and Medicine, Albert Einstein College of Medicine, Bronx, New York, USA

Twitter Chloé Michaudel @ChloeMichaudel, Julien Kirchgesner @J_Kirchgesner and Harry Sokol @h_sokol

Acknowledgements Nanostring—The authors thank the UMR 8199 LIGAN-MP Genomics platform (Lille, France) which belongs to the 'Federation de Recherche' 3508 Labex EGID (European Genomics Institute for Diabetes; ANR-10-LABX-46). Histology and Bioanalyser- This work has benefited from the facilities and expertise of @BRIDGe (Université Paris-Saclay, INRAE, AgroParisTech, GABI, 78350 Jouy-en-Josas, France). Mice-The authors thanks Tatiana Ledent and IERP team, for breeding.

Contributors CM performed the majority of the experiments. CD, AM, AAu, AAg, MS, YW, AoL, CG, GDC, MP, AnL, JP, CO, LC, LGB-H and PL contributed and/or supported us for some experiments. AL and PE performed/contributed to trp metabolites dosages. JK, NB, AB, IN-L, CL, PS and LB provided/analyzed human material/samples. RRA provided SCENITH assay. CM and HS designed the study and wrote the manuscript. PN, PI and ZD performed ligand-binding assay. CM, HS, ZD, LGB-H, PL, DM, SM, MLR, PE, NR and M-LM read the manuscript and contributed to the finalised version. All authors approved the final version of the manuscript. HS was responsible for the overall content as the guarantor.

Funding HS received funding from the European Research Council (ERC) under the European Union's Horizon 2020 Research and Innovation Programme (ERC-2016-StG-71577) and from Agence Nationale de Recherche (ANR-20-CE14-0005-1). HS and NR received funding from Association Francois Aupetit (AFA). ZD received financial support grant from Czech Science Foundation, No 20-00449S.

Competing interests HS report lecture fee, board membership, or consultancy from Carenity, AbbVie, Astellas, Danone, Ferring, Mayoly Spindler, MSD, Novartis, Roche, Tillots, Enterome, BiomX, Biose, Novartis,Takeda, Biocodex and is cofounder of Exeliom Biosciences.

Patient and public involvement Patients and/or the public were not involved in the design, or conduct, or reporting, or dissemination plans of this research.

Patient consent for publication Not applicable.

Ethics approval This study involves human participants and was approved by Comité de Protection des Personnes Ile-de-France IV, IRB 00003835 Suivitheque study; registration number 2012/05NICB. Participants gave informed consent to participate in the study before taking part.

Provenance and peer review Not commissioned; externally peer reviewed.

Data availability statement Data are available on reasonable request.

ORCID iDs
Julien Kirchgesner http://orcid.org/0000-0002-2314-9284
David Moulin http://orcid.org/0000-0001-6619-5769
Harry Sokol http://orcid.org/0000-0002-2914-1822

REFERENCES
1 Furman D, Campisi J, Verdin E, *et al*. Chronic inflammation in the etiology of disease across the life span. *Nat Med* 2019;25:1822–32.
2 Xu X-R, Liu C-Q, Feng B-S, *et al*. Dysregulation of mucosal immune response in pathogenesis of inflammatory bowel disease. *World J Gastroenterol* 2014;20:3255.
3 Lamas B, Richard ML, Leducq V, *et al*. Card9 impacts colitis by altering gut microbiota metabolism of tryptophan into aryl hydrocarbon receptor ligands. *Nat Med* 2016;22:598–605.
4 Sartor RB, Wu GD. Roles for intestinal bacteria, viruses, and fungi in pathogenesis of inflammatory bowel diseases and therapeutic approaches. *Gastroenterology* 2017;152:327–39.
5 Burger JR, Hou C, Brown JH. Toward a metabolic theory of life history. *Proc Natl Acad Sci U S A* 2019;116:26653–61.
6 Pols T, Sikkema HR, Gaastra BF, *et al*. A synthetic metabolic network for physicochemical homeostasis. *Nat Commun* 2019;10:4239.
7 Duddu AS, Sahoo S, Hati S, *et al*. Multi-stability in cellular differentiation enabled by a network of three mutually repressing master regulators. *J. R. Soc. Interface.* 2020;17:20200631.
8 Lampropoulou V, Sergushichev A, Bambouskova M, *et al*. Itaconate links inhibition of succinate dehydrogenase with macrophage metabolic remodeling and regulation of inflammation. *Cell Metab* 2016;24:158–66.
9 Pavlova NN, Thompson CB. The emerging hallmarks of cancer metabolism. *Cell Metab* 2016;23:27–47.
10 Nikolaus S, Schulte B, Al-Massad N, *et al*. Increased tryptophan metabolism is associated with activity of inflammatory bowel diseases. *Gastroenterology* 2017;153:1504–16.
11 Agus A, Planchais J, Sokol H. Gut microbiota regulation of tryptophan metabolism in health and disease. *Cell Host Microbe* 2018;23:716–24.

12 Dodd D, Spitzer MH, Van Treuren W, *et al*. A gut bacterial pathway metabolizes aromatic amino acids into nine circulating metabolites. *Nature* 2017;551:648–52.
13 Manzella CR, Jayawardena D, Pagani W, *et al*. Serum serotonin differentiates between disease activity states in Crohn's patients. *Inflamm Bowel Dis* 2020;26:1607–18.
14 Tashita C, Hoshi M, Hirata A, *et al*. Kynurenine plays an immunosuppressive role in 2,4,6-trinitrobenzene sulfate-induced colitis in mice. *World J Gastroenterol* 2020;26:918–32.
15 Cussotto S, Delgado I, Anesi A, *et al*. Tryptophan metabolic pathways are altered in obesity and are associated with systemic inflammation. *Front Immunol* 2020;11:557.
16 Hubbard TD, Murray IA, Perdew GH. Indole and tryptophan metabolism: endogenous and dietary routes to Ah receptor activation. *Drug Metab Dispos* 2015;43:1522–35.
17 Agudelo LZ, Ferreira DMS, Cervenka I, *et al*. Kynurenic acid and GPR35 regulate adipose tissue energy homeostasis and inflammation. *Cell Metab* 2018;27:378–92.
18 Lugo-Huitrón R, Ugalde Muñiz P, Pineda B, *et al*. Quinolinic acid: an endogenous neurotoxin with multiple targets. *Oxid Med Cell Longev* 2013;2013:1–14.
19 Campesato LF, Budhu S, Tchaicha J, *et al*. Blockade of the AhR restricts a Treg-macrophage suppressive axis induced by L-kynurenine. *Nat Commun* 2020;11:4011.
20 Quintana FJ, Basso AS, Iglesias AH, *et al*. Control of Treg and Th17 cell differentiation by the aryl hydrocarbon receptor. *Nature* 2008;453:65–71.
21 McAleer JP, Fan J, Roar B, *et al*. Cytokine regulation in human CD4 T cells by the aryl hydrocarbon receptor and Gq-coupled receptors. *Sci Rep* 2018;8:10954.
22 Michaudel C, Bataille F, Maillet I, *et al*. Ozone-Induced aryl hydrocarbon receptor activation controls lung inflammation via interleukin-22 modulation. *Front Immunol* 2020;11:144.
23 Schiering C, Wincent E, Metidji A, *et al*. Feedback control of AhR signalling regulates intestinal immunity. *Nature* 2017;542:242–5.
24 Vogel CFA, Van Winkle LS, Esser C, *et al*. The aryl hydrocarbon receptor as a target of environmental stressors – implications for pollution mediated stress and inflammatory responses. *Redox Biol* 2020;34:101530.
25 Sokol H, Landman C, Seksik P, *et al*. Fecal microbiota transplantation to maintain remission in Crohn's disease: a pilot randomized controlled study. *Microbiome* 2020;8:12.
26 Wisniewski A, Kirchgesner J, Seksik P, *et al*. Increased incidence of systemic serious viral infections in patients with inflammatory bowel disease associates with active disease and use of thiopurines. *United European Gastroenterol J* 2020;8:303–13.
27 Metidji A, Omenetti S, Crotta S, *et al*. The environmental sensor AhR protects from inflammatory damage by maintaining intestinal stem cell homeostasis and barrier integrity. *Immunity* 2018;49:353–62.
28 Yin J, Sheng B, Qiu Y, *et al*. Role of AhR in positive regulation of cell proliferation and survival. *Cell Prolif* 2016;49:554–60.
29 Michaudel C, Sokol H. The gut microbiota at the service of Immunometabolism. *Cell Metab* 2020;32:514–23.
30 Argüello RJ, Combes AJ, Char R, *et al*. SCENITH: a flow cytometry-based method to functionally profile energy metabolism with single-cell resolution. *Cell Metab* 2020;32:1063–75.
31 Alarcan H, Chaumond R, Emond P, *et al*. Some CSF kynurenine pathway intermediates associated with disease evolution in amyotrophic lateral sclerosis. *Biomolecules* 2021;11:691.
32 Gálvez J. Role of Th17 cells in the pathogenesis of human IBD. *ISRN Inflamm* 2014;2014:1–14.
33 Kinugasa T, Sakaguchi T, Gu X, *et al*. Claudins regulate the intestinal barrier in response to immune mediators. *Gastroenterology* 2000;118:1001–11.
34 Kirchner FR, LeibundGut-Landmann S. Tissue-Resident memory Th17 cells maintain stable fungal commensalism in the oral mucosa. *Mucosal Immunol* 2021;14:455–67.
35 Hueber W, Sands BE, Lewitzky S, *et al*. Secukinumab, a human anti-IL-17A monoclonal antibody, for moderate to severe Crohn's disease: unexpected results of a randomised, double-blind placebo-controlled trial. *Gut* 2012;61:1693–700.
36 Yansen Z, Lingang Z, Dali L. Inflammatory bowel disease susceptible gene GPR35 promotes bowel inflammation in mice. *Yi Chuan* 2021;43:169–81.
37 Walczak K, Langner E, Makuch-Kocka A, *et al*. Effect of tryptophan-derived AhR ligands, kynurenine, kynurenic acid and FICZ, on proliferation, cell cycle regulation and cell death of melanoma Cells—In vitro studies. *Int J Mol Sci* 2020;21:E7946.
38 Donohoe DR, Garge N, Zhang X, *et al*. The microbiome and butyrate regulate energy metabolism and autophagy in the mammalian colon. *Cell Metab* 2011;13:517–26.
39 Skelly AN, Sato Y, Kearney S, *et al*. Mining the microbiota for microbial and metabolite-based immunotherapies. *Nat Rev Immunol* 2019;19:305–23.
40 Gill R, Woodruff GN. The neuroprotective actions of kynurenic acid and MK-801 in gerbils are synergistic and not related to hypothermia. *Eur J Pharmacol* 1990;176:143–9.
41 Dupraz L, Magniez A, Rolhion N, *et al*. Gut microbiota-derived short-chain fatty acids regulate IL-17 production by mouse and human intestinal γδ T cells. *Cell Rep* 2021;36:109332.
42 Sokol H, Conway KL, Zhang M, *et al*. Card9 mediates intestinal epithelial cell restitution, T-helper 17 responses, and control of bacterial infection in mice. *Gastroenterology* 2013;145:591–601.
43 Lefèvre A, Mavel S, Nadal-Desbarats L, *et al*. Validation of a global quantitative analysis methodology of tryptophan metabolites in mice using LC-MS. *Talanta* 2019;195:593–8.
44 Denison MS, Rogers JM, Rushing SR, *et al*. Analysis of the Aryl Hydrocarbon Receptor (AhR) Signal Transduction Pathway. *Curr Protoc Toxicol* 2002;11.

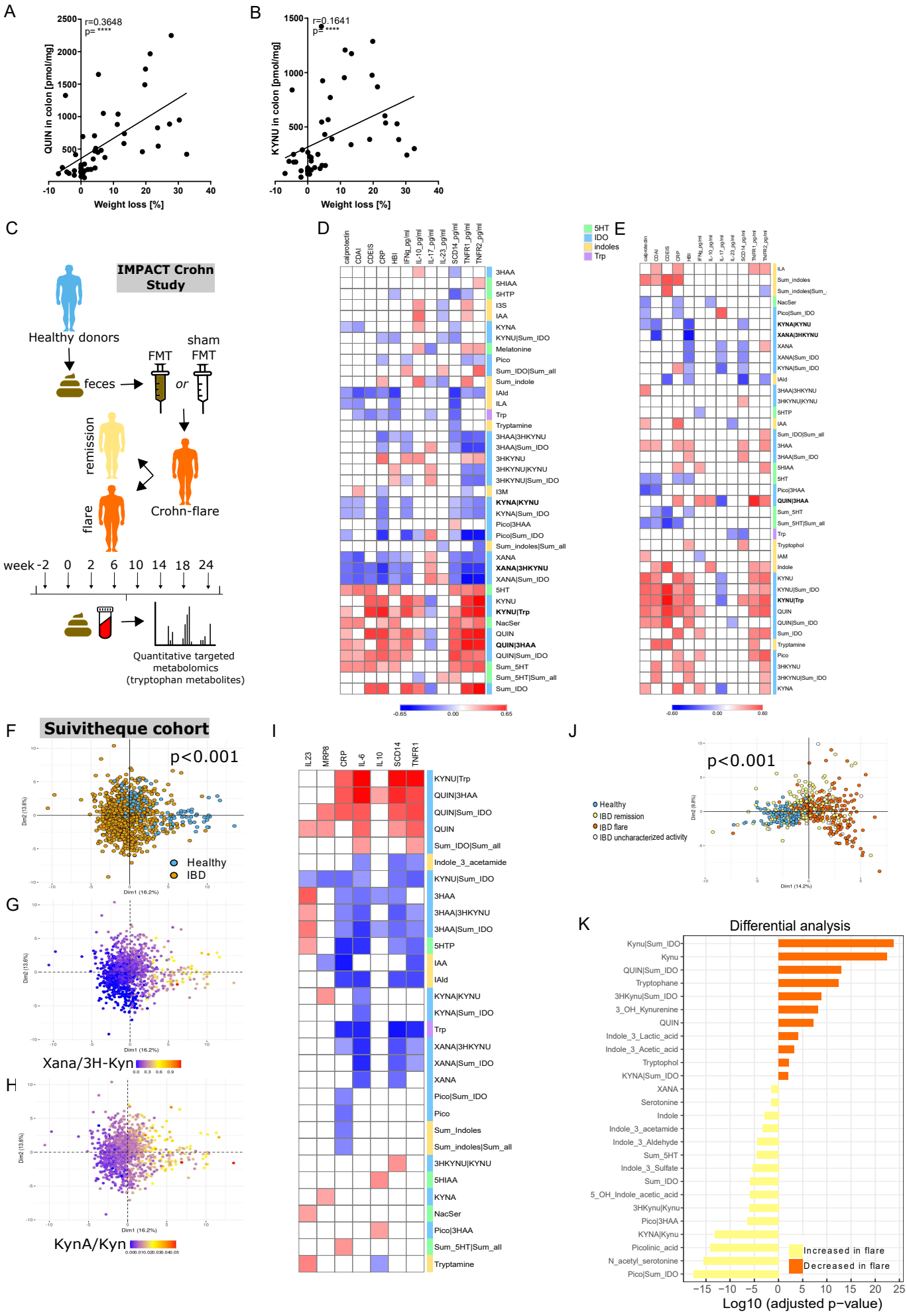
A
r=0.3648
p= ****
QUIN in colon [pmol/mg]
Weight loss [%]
B
r=0.1641
p= ****
KYNU in colon [pmol/mg]
Weight loss [%]
C
IMPACT Crohn Study
Healthy donors
feces
FMT
or
sham FMT
remission
flare
Crohn-flare
week -2 0 2 6 10 14 18 24
Quantitative targeted metabolomics (tryptophan metabolites)
D
E
5HT
IDO
indoles
Trp
F
Suivitheque cohort
p<0.001
Healthy
IBD
G
Xana/3H-Kyn
H
KynA/Kyn
I
J
p<0.001
Healthy
IBD remission
IBD flare
IBD uncharacterized activity
K
Differential analysis
Kynu|Sum_IDO
Kynu
QUIN|Sum_IDO
Tryptophane
3HKynu|Sum_IDO
3_OH_Kynurenine
QUIN
Indole_3_Lactic_acid
Indole_3_Acetic_acid
Tryptophol
KYNA|Sum_IDO
XANA
Serotonine
Indole
Indole_3_acetamide
Indole_3_Aldehyde
Sum_5HT
Indole_3_Sulfate
Sum_IDO
5_OH_Indole_acetic_acid
3HKynu|Kynu
Pico|3HAA
KYNA|Kynu
Picolinic_acid
N_acetyl_serotonine
Pico|Sum_IDO
Increased in flare
Decreased in flare
Log10 (adjusted p−value)

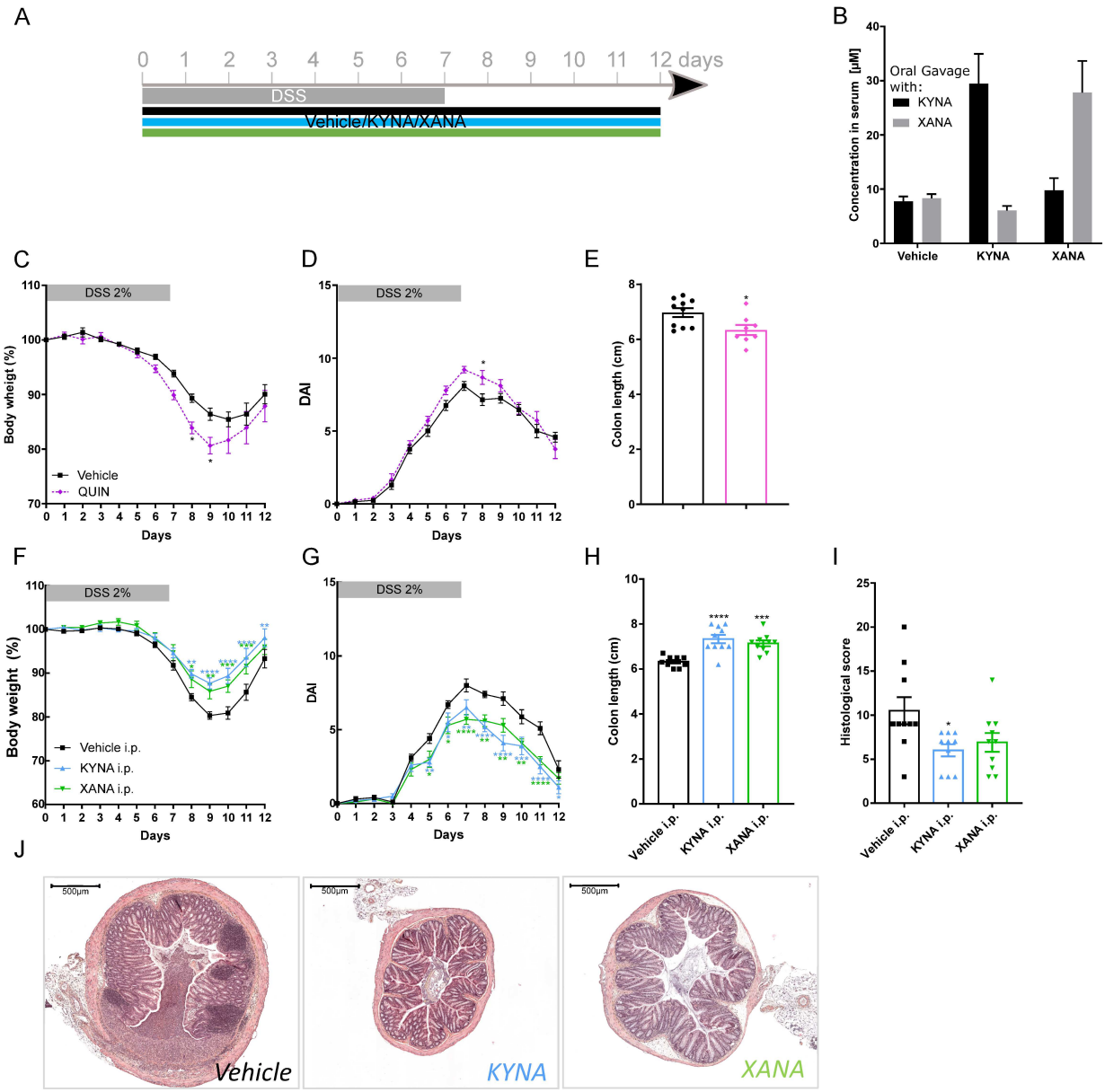
A
0 1 2 3 4 5 6 7 8 9 10 11 12 days
DSS
Vehicle/KYNA/XANA
B
Concentration in serum [µM]
Oral Gavage with:
KYNA
XANA
Vehicle
KYNA
XANA
C
DSS 2%
Body wheigt (%)
Vehicle
QUIN
Days
D
DSS 2%
DAI
Days
E
Colon length (cm)
F
DSS 2%
Body weight (%)
Vehicle i.p.
KYNA i.p.
XANA i.p.
Days
G
DSS 2%
DAI
Days
H
Colon length (cm)
Vehicle i.p.
KYNA i.p.
XANA i.p.
I
Histological score
Vehicle i.p.
KYNA i.p.
XANA i.p.
J
500µm
Vehicle
KYNA
XANA

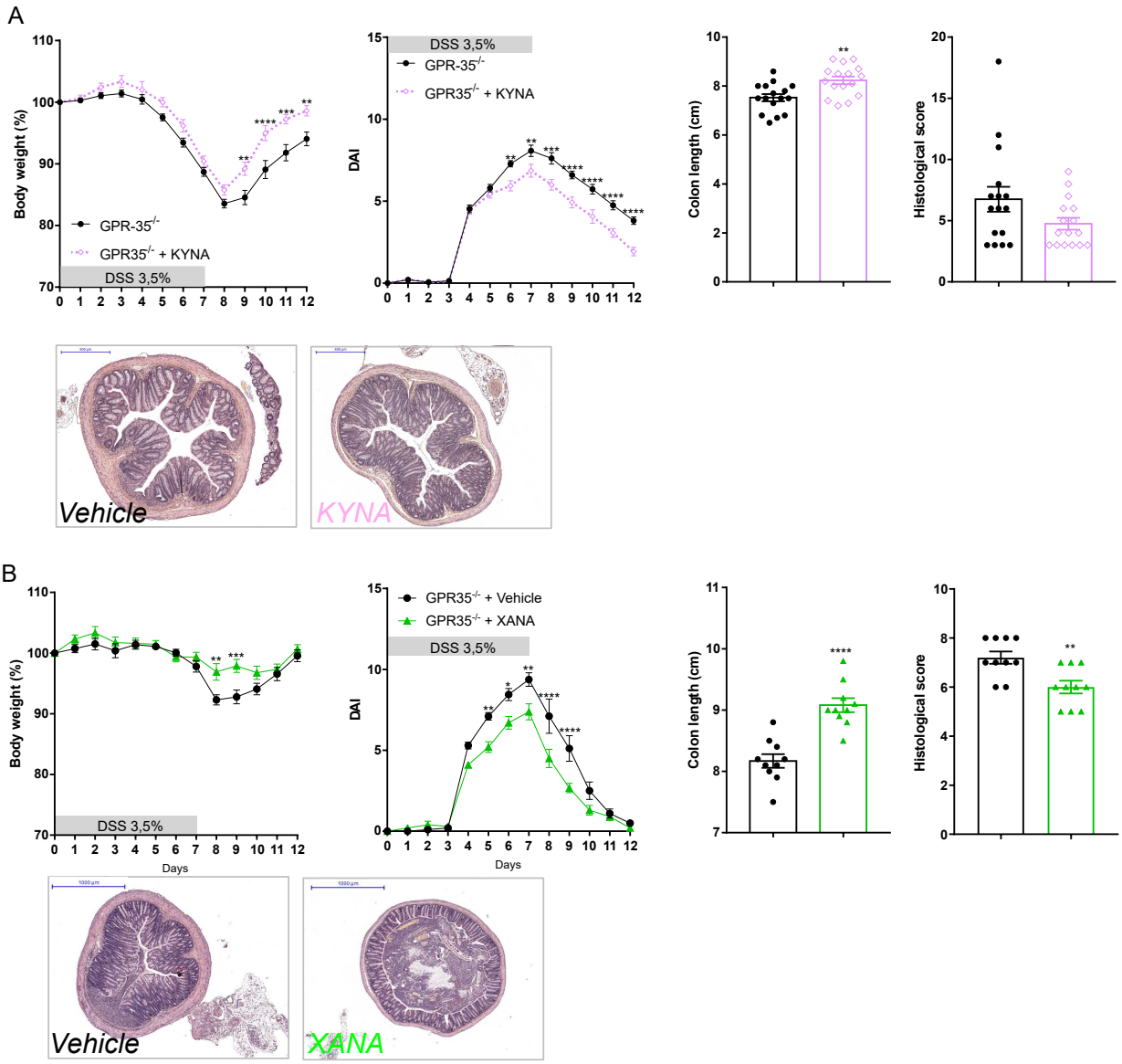
A
Body weight (%)
GPR-35-/-
GPR35-/- + KYNA
DSS 3,5%
DAI
Colon length (cm)
Histological score
Vehicle
KYNA
B
GPR35-/- + Vehicle
GPR35-/- + XANA
Days
Vehicle
XANA

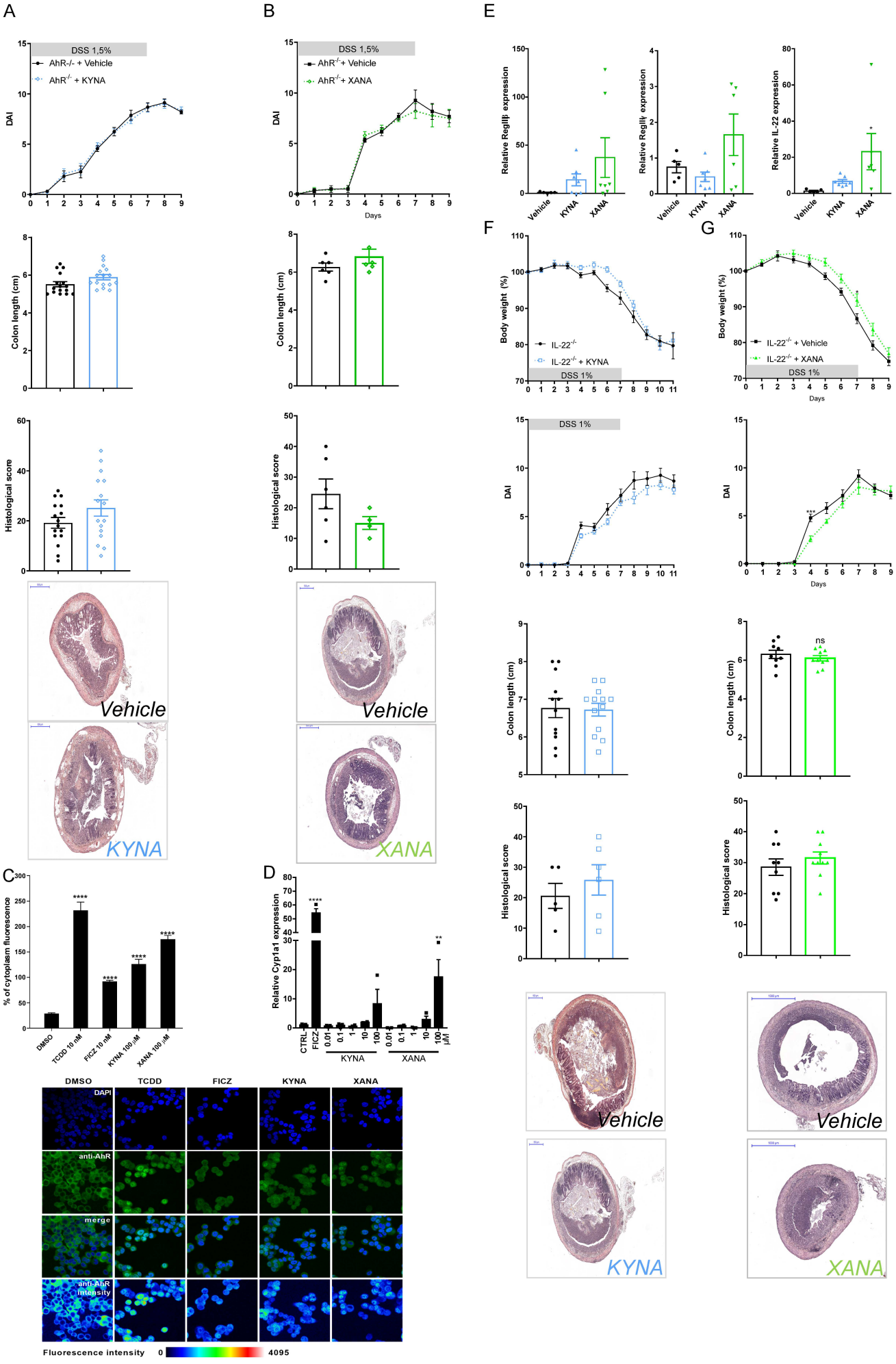
A
DSS 1,5%
AhR-/- + Vehicle
AhR-/- + KYNA
DAI
Colon length (cm)
Histological score
Vehicle
KYNA
B
DSS 1,5%
AhR-/- + Vehicle
AhR-/- + XANA
Days
Colon length (cm)
Histological score
Vehicle
XANA
C
% of cytoplasm fluorescence
DMSO
TCDD 10 nM
FICZ 10 nM
KYNA 100 µM
XANA 100 µM
DMSO
TCDD
FICZ
KYNA
XANA
DAPI
anti-AhR
merge
anti-AhR Intensity
Fluorescence intensity 0 4095
D
Relative Cyp1a1 expression
CTRL
FICZ
KYNA
XANA
µM
E
Relative RegIIIβ expression
Relative RegIIIγ expression
Relative IL-22 expression
Vehicle
KYNA
XANA
F
Body weight (%)
IL-22-/-
IL-22-/- + KYNA
DSS 1%
DAI
Colon length (cm)
Histological score
Vehicle
KYNA
G
Body weight (%)
IL-22-/- + Vehicle
IL-22-/- + XANA
DSS 1%
Days
DAI
Colon length (cm)
ns
Histological score
Vehicle
XANA

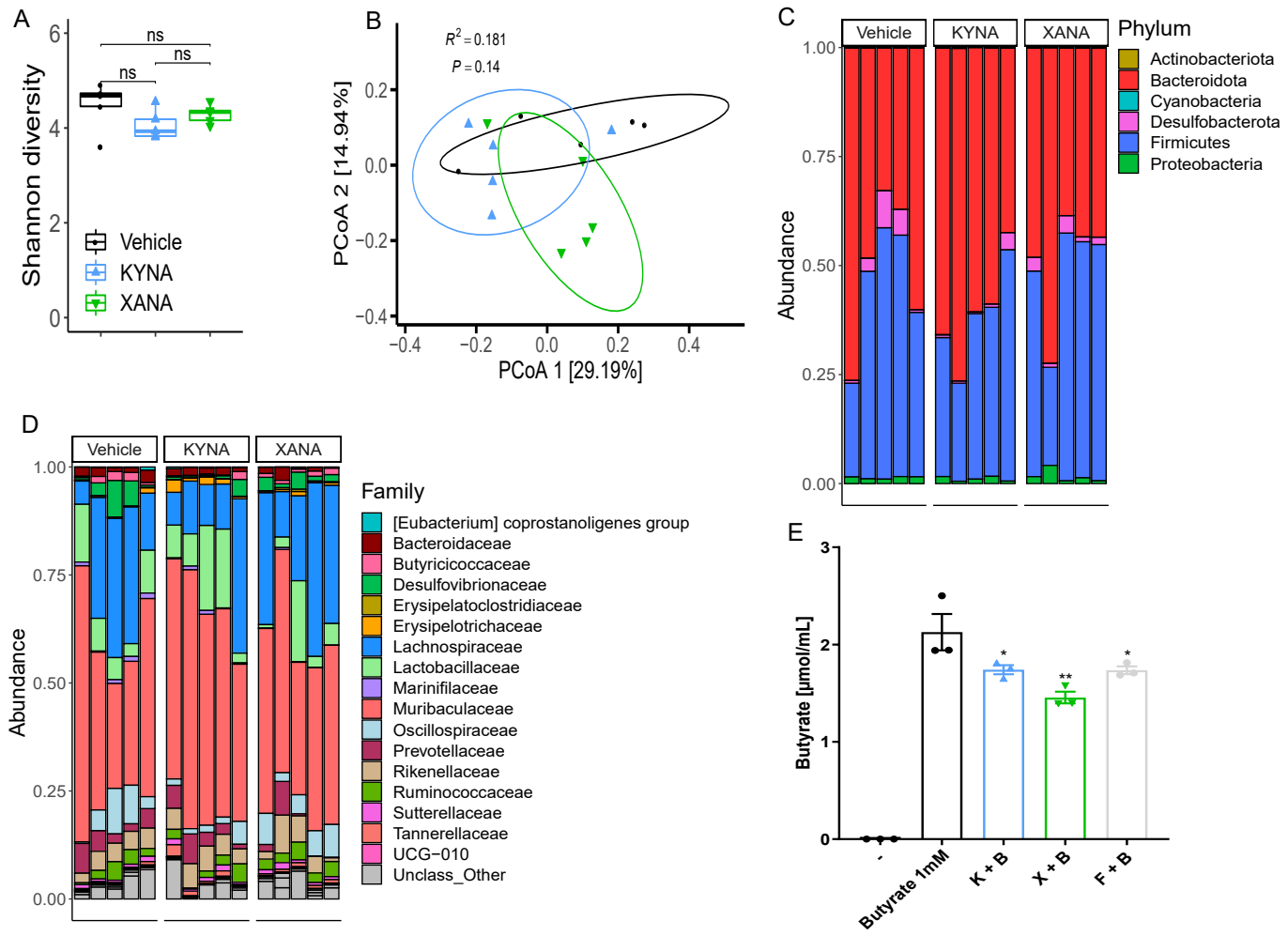
A
Shannon diversity
ns
ns
ns
Vehicle
KYNA
XANA
B
R^2 = 0.181
P = 0.14
PCoA 2 [14.94%]
PCoA 1 [29.19%]
C
Vehicle
KYNA
XANA
Phylum
Actinobacteriota
Bacteroidota
Cyanobacteria
Desulfobacterota
Firmicutes
Proteobacteria
Abundance
D
Vehicle
KYNA
XANA
Family
[Eubacterium] coprostanoligenes group
Bacteroidaceae
Butyricicoccaceae
Desulfovibrionaceae
Erysipelatoclostridiaceae
Erysipelotrichaceae
Lachnospiraceae
Lactobacillaceae
Marinifilaceae
Muribaculaceae
Oscillospiraceae
Prevotellaceae
Rikenellaceae
Ruminococcaceae
Sutterellaceae
Tannerellaceae
UCG−010
Unclass_Other
Abundance
E
Butyrate [µmol/mL]
-
Butyrate 1mM
K + B
X + B
F + B

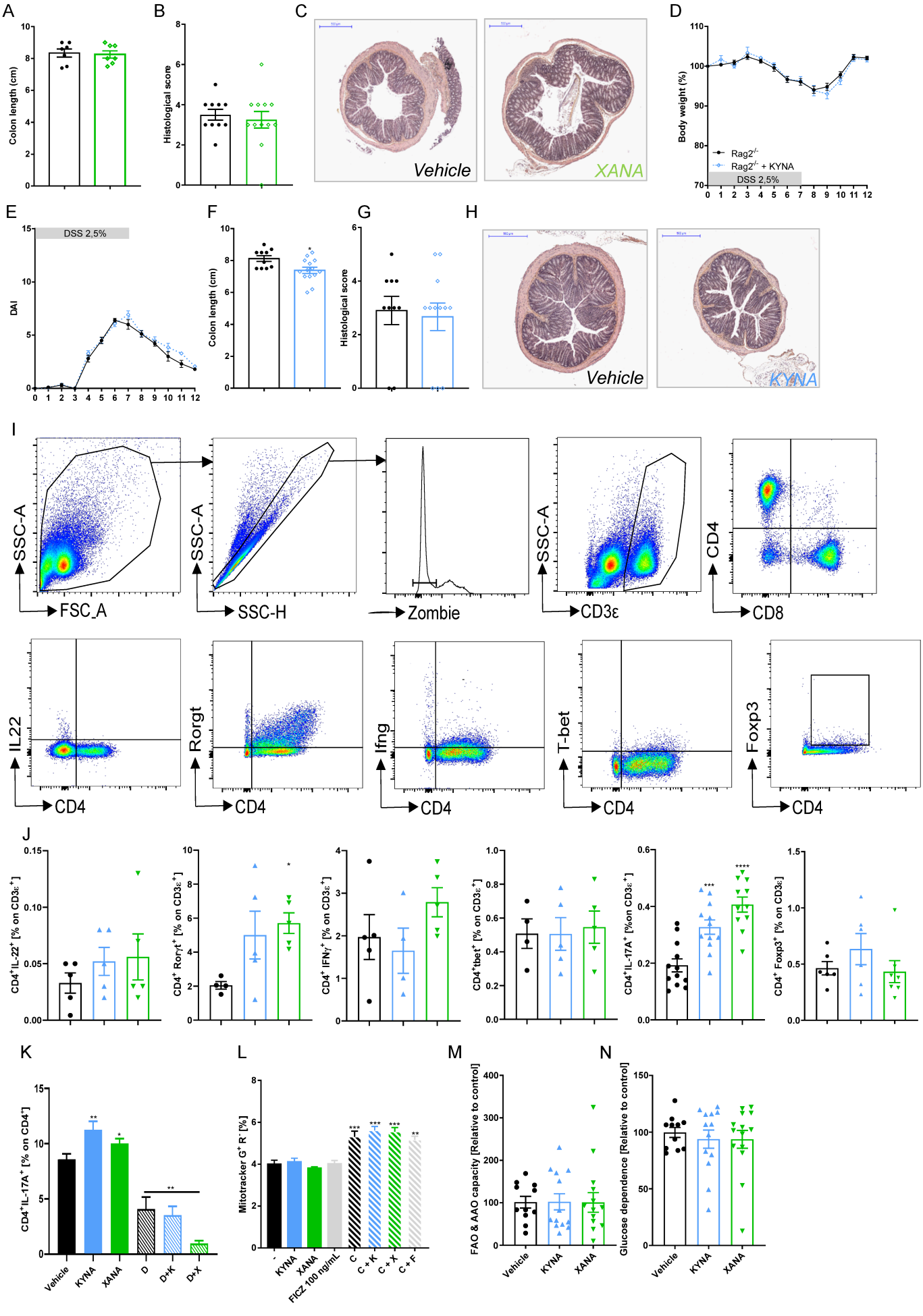
A
Colon length (cm)
B
Histological score
C
Vehicle
XANA
D
Body weight (%)
Rag2-/-
Rag2-/- + KYNA
DSS 2,5%
E
DSS 2,5%
DAI
F
Colon length (cm)
G
Histological score
H
Vehicle
KYNA
I
SSC-A
FSC_A
SSC-H
Zombie
CD3ε
CD4
CD8
IL22
Rorgt
Ifng
T-bet
Foxp3
J
CD4+IL-22+ [% on CD3ε+]
CD4+ Rorγt+ [% on CD3ε+]
CD4+ IFNγ+ [% on CD3ε+]
CD4+tbet+ [% on CD3ε+]
CD4+IL-17A+ [%on CD3ε+]
CD4+ Foxp3+ [% on CD3ε]
K
CD4+IL-17A+ [% on CD4+]
Vehicle
KYNA
XANA
D
D+K
D+X
L
Mitotracker G+ R- [%]
FICZ 100 ng/mL
C
C + K
C + X
C + F
M
FAO & AAO capacity [Relative to control]
N
Glucose dependence [Relative to control]

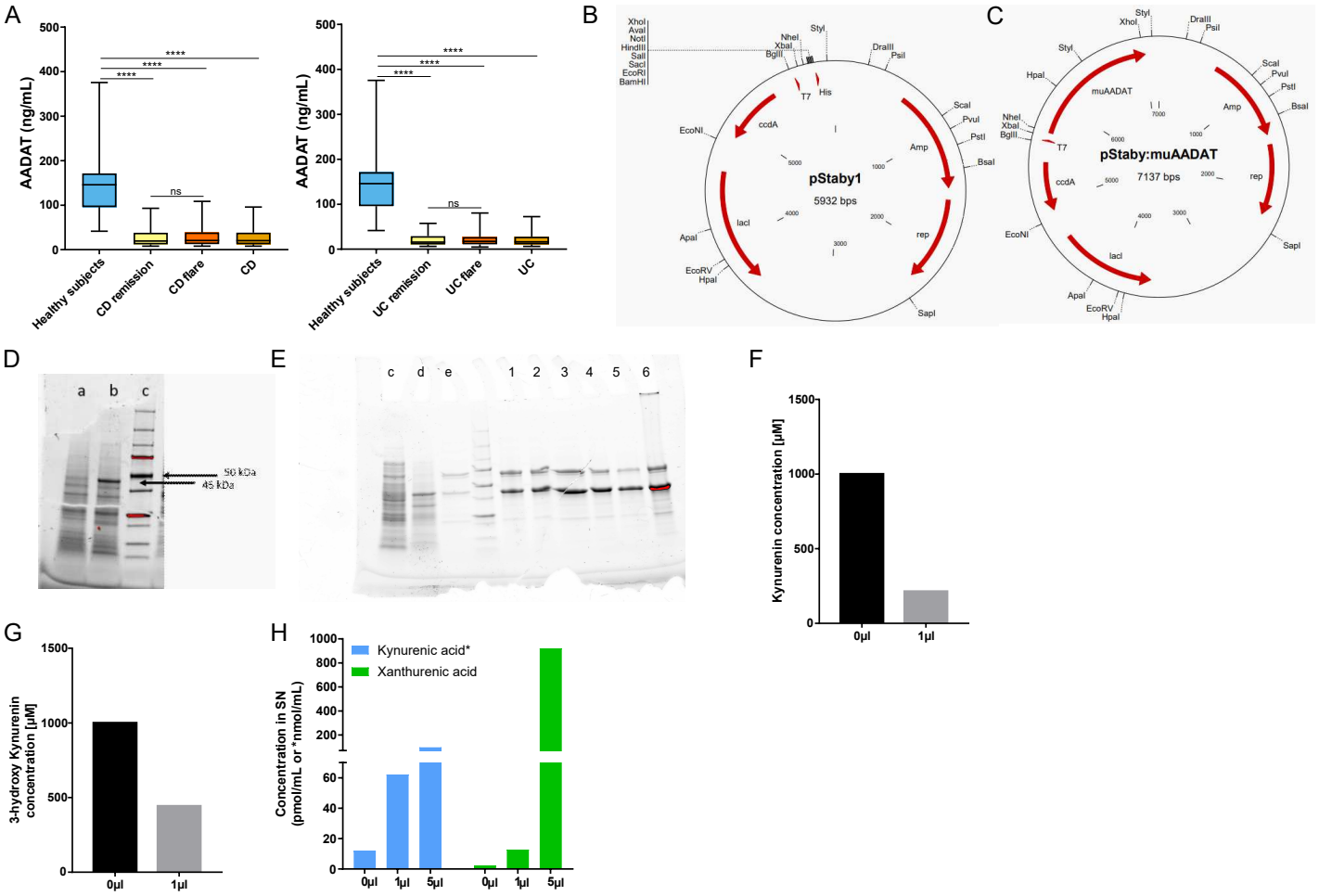
A
AADAT (ng/mL)
Healthy subjects
CD remission
CD flare
CD
UC remission
UC flare
UC
ns
****
B
pStaby1
5932 bps
C
pStaby:muAADAT
7137 bps
muAADAT
D
a
b
c
50 kDa
45 kDa
E
c
d
e
1
2
3
4
5
6
F
Kynurenin concentration [µM]
0µl
1µl
G
3-hydroxy Kynurenin concentration [µM]
H
Concentration in SN (pmol/mL or *nmol/mL)
Kynurenic acid*
Xanthurenic acid
0µl
1µl
5µl

Supplementary Material and methods

Cell lines

HT-29 (ATCC), a human intestinal epithelial cell line, was grown in DMEM supplemented with 10% FCS and PS. Jurkat (ATCC Clone E6-1), a human T cell line, was grown in RPMI supplemented with 10% FCS and PS. LS180 cells (ECACC), a human intestinal epithelial cell line, were grown in DMEM supplemented with 10% FCS.

Mouse Model

All the experiments were performed in the specific pathogen-free animal facility at IERP (INRAe, Jouy-en-Josas, agreement C78-720), in a temperature-controlled environment and with a strict 12h light/dark cycle. WT mice were obtained from Janvier lab, IL-22$^{-/-}$ [44] from TAAM Orléans, AhR$^{-/-}$ [45], Rag2$^{-/-}$ and AhR$^{\Delta IEC}$ from St Antoine research center animal facility (UMR S938, PHEA), and GPR35$^{-/-}$ [46] from IERP.

IBD cohorts

All individuals from the Suivitheque study were recruited in the Gastroenterology Department of the Saint Antoine Hospital (Paris, France) and provided informed consent. All samples were obtained between June 2012 and November 2019. The clinical activity reported in Figure 2F was previously described [47]**. Briefly:** at each contact in the IBD unit, clinical activity is scored prospectively as follows: 0, no digestive symptoms; 1, mild symptoms that may be attributable to IBD activity, postoperative functional sequelae or associated irritable bowel syndrome; 2, symptoms that are attributable to IBD and are compatible with usual home and/or professional activities; 3, symptoms that are attributable to IBD and are not compatible with sustained home and/or professional activities; 4, hospitalization for IBD flare; 5, intestinal resection. Remission is defined by a score of 0 or 1.

Seahorse

Following drugs concentrations were used: for Mito stress assay – Olygomycin (Olygo) 1.5µM, FCCP 1µM and Rotenone/Antimycin A (Rot/AA) 0.5µM; for Glycolityc rate assay - Rot/AA 0.5µM and 2-DG 50µM. For basal measurement and each injection, following program is repeat three times– injection compound, mixing (3min), waiting (5min), measuring (3min). Oxygen Consumption Rate (OCR, using the Mito Stress Test kit) and Extracellular Flux Analyser (ECAR, using the Glycolytic Rate Assay kit) were measured. Total protein amount was quantified with DC protein assay (BioRad, 500113-114) and used to normalize values. Analysis were performed with Wave software.

DSS-induced colitis model

In all experiments, body weight, blood in stool, and stool consistency were analyzed daily. The severity of colitis was assessed using the disease activity index (DAI), and, at day twelve, colon length and histological scoring as previously described [3].

Nanostring

All samples had a RIN≥8. After control, RNA was diluted at 15ng/µL. XT_PGX_MmV1 Immunology kit was used following manufacturer's instruction with 250ng per sample, prepared with nCounterPrep Station and read with nCounterPrep Analyzer thanks to Immunology Mm C2269 panel. Data were analyzed with NSolver software.

Scratch test

HT-29 cells were plated at 100,000 cells per chamber in 80µL of DMEM supplemented with 10% FCS and P/S. When cells were confluent, chambers were removed, and stimulation was performed with KYNA (100µM), XANA (100µM) and FICZ (0.2pg/µL) with or without CH223191 (Sigma, 10µM), for 72h. Each dish was pictured with a ZEISS microscope and analyzed with Zen and ImageJ software. Each wound was measured on full length 60 times minimum. Oligomycin (Sigma) is used at 5µM.

Organoids

For mouse organoids, colon was prepared and cleaned with washing solution (1X DPBS + 10% SVF + 2% Penicillin/streptomycin + 1% Gentamycin). Dissociation solution (1X DPBS + 8mM EDTA) was used for 15 and 30 min to harvest crypts. Crypts were resuspended and counted in DMEM/F12 completed + 2% Penicillin/Streptomycin. Fifty crypts were then seeded per well in 1:2 DMEM/F12 (supplemented with Glutamax 1X (Gibco), Penicillin/Streptomycin 1X (Gibco), HEPES 1X (Gibco), N2 1X (Gibco), B27 (Gibco), murine EGF 50ng/mL (Peprotech), recombinant mouse Noggin 100ng/mL (R&D), recombinant mouse R-Spondin1 CF 500ng/mL (R&D), mWnt-3a 100ng/mL (R&D) and CHIR99021 3µM (Peprotech)) and matrigel (Corning) or Ultimatrix (R&D).

Fifty crypts were then seeded per well in 1:2 DMEM/F12 (Supplemented with Glutamax 2m, HEPES 10mM, N2 1X (Thermofosher), human R-Spondin 1µg/mL (R&D), Nicotinamide 10mM (Sigma), B27/Vitamin A 1X (Thermofisher), human Noggin 100ng/mL (R&D), human EGF 50ng/mL (R&D), N-acetylcysteine 1mM (Sigma), Gastrin 10nM (Sigma), SB202190 10µM (Sigma), PGE2 0.01µM (Sigma), LY2157299 0.5nM (Sigma) and Wnt3a 0.5nM (R&D)) and matrigel (Corning) or Ultimatrix (R&D). Organoids were used seven days later and were treated with vehicle, KYNA (100µM) and XANA (100µM) with or without oligomycin (5µM) during 72h.

Edu proliferation assay

Click-iT® EdU flow cytometry assay kit (Invitrogen, C10425) was used according to manufacturer's instructions..

qPCR Analysis

The oligonucleotides used were as follows: Smct (F_ ATGCATTCGTCTCTGTGGCA R_CTGCTTTAAGACCGCCCAGT), Mct-1 (F_CATTGGTGTTATTGGAGGTC R_GAAAGCCTGATTAAGTGGAG), Rorc (F_TGGCTGCAAAGAAGACCCAC R_CCCACATTGACTTCCTCTGGT), Ifnγ (F_CCATCCTTTTGCCAGTTCCTC R_ATGAACGCTACACACTGCATC), Il1β (F_GCCCATCCTCTGTGACTCAT, R_AG-

GCCACAGGTATTTTGTCG), RegIIIγ (F_TTCCTGTCCTCCATGATCAAAA R_CATCCAC-CTCTGTTGGGTTCA), RegIIIβ (F_ATGCTGCTCTCCTGCCTGATG R_CTAATGCGTGCG-GAGGGTATATTC), IL-22 (F_CATGCAGGAGGTGGTGCCTT R_CAGACGCAA-GCATTTCTCAG), Lcn2 (*Qiagen, QuantiTect GT00113407*), and Cyp1a1 (*Qiagen, QuantiTect QT00105756*). We used the 2−ΔΔ*Ct* quantification method with mouse *Hprt1 (Qiagen, QuantiTect QT00166768)* as endogenous control and the WT group as a calibrator. For human cells, we used Cyp1a1 (F_CAGCTCAGCTCAGTACCTCA R_CTTGAGGCCCTGATTACCCA) and Gapdh (F_AAGTGGTCGTTGAGGGCAATG R_CTGGGCTACACTGAGCACC.

Histology

Colon samples for histological studies were maintained at 4°C in 4% paraformaldehyde and then embedded in paraffin. 4-µm sections (three sections per sample) were stained with hematoxylin and eosin (H&E) and then examined in a blinded manner using a BX43 Olympus microscope to determine the histological score, as described previously [41].

Immunofluorescence staining was performed according to standard staining methods on a Leica BOND RX^{m}, including a deparaffinization and rehydration step, an alkaline antigen retrieval step (20min at 100˚C in Bond^{TM} Epitope Retrieval 2, *AR9640*), and blocking with 1% BSA and 10% Normal Goat Serum for 30min at room temperature.

Primary antibody anti-Ki67 (dilution 1/500, Abcam, ab15580) was applied on slides 1h at room temperature, followed by secondary antibody (dilution 1/2300, Invitrogen, *A11011*) with DAPI for 30 min at room temperature. Slides were mounted with Fluoromount ® (Cliniscience, *0100-01*). Slides were scanned using the Pannoramic SCAN II automated slide scanner (3D HISTECH) at 20X.

FACS

All extracellular staining were realized in FACS Buffer (PBS1X + EDTA 0.5mM + FCS 2%). Staining beginning each time with a viability dye, either Fixable Viability Dye (*eBioscience*) or

Zombie Aqua Fixable Viability Kit (*Biolegend*). Cells were surface stained in FACS buffer with the following antibodies: C16/CD32 (*eBioscience,* 14-0161-85), CD45 (*Biolegend 103147*), CD4 (*Biolegend 100552*), EpCAM (*Biolegend* 118205) and CD3ε (*eBioscience 11-0031-82*). For cytokines, cells were stimulated during 2 hours by PMA (50ng/mL) and ionomycin (1µg/mL) plus IL-1β (10ng/mL), IL-23 (20ng/mL) and Brefeldin-A (10µg/mL) before staining. For intracellular staining Cytofix/Cytoperm (*BD*) or Factor staining buffer Set (*eBioscience, 00-5523-00*) were used following manufacturer's protocols with following antibodies: IL-17A (*Biolegend 506914*), rorγt (*eBioscience 12-6988-82*), tbet (*Biolegend 644817*), foxp3 (*eBioscience 48-5773-82*), IFNγ (*Biolegend 505850*) and IL-22 (*eBioscience, 46-7221-82*). All data are acquired with LSR Fortessa X-20 (*BD Biosciences*) and analyzed with FlowJo software.

T cell differentiation

24-well plates were coated overnight with 2µg/mL of αCD3 and 10µg/mL of αCD28. Cells from WT spleen were prepared, minced and red blood cells were lysed with a red blood lysis solution. Naïve CD4 T cells were sorted with Milteny kit (130-104-453), following manufacturer instructions. 500,000 cells were plated per well. For T_H17, naïve CD4 T cells were incubated with IL-6 (0.1mg/mL) and TGFβ (0.2mg/mL) with KYNA (100µM), XANA (100µM) with or without CH223191 (Sigma, 10µM) during 72h. After incubation, cells were stained, with αCD4, αIL-17A, αRorγt and viability dye, and the level of differentiation was compared with LSF Fortessa X20. 2DG (*Sigma, D6134*) was used at 10mM.

16S sequencing analysis

Fecal DNA extraction was performed as previously described [3]. Gut microbiota composition and diversity were determined using 16S sequencing. Following PCR (V3-V4 region, PCR1F_460: 5' CTTTCCCTACACGACGCTCTTCCGATCTACGGRAGGCAGCAG 3', PCR1R_460: 5' GGAGTTCAGACGTGTGCTCTTCCGATCTTACCAGGGTATCTAATCCT 3'), amplicon quality was verified by gel electrophoresis and sent to the @BRIDGe plateform

for sequencing protocol on an Illumina MiSeq (Illumina, San Diego, CA, USA). The dada2 software package (version 1.14.1)[48] in the R programming language (R version 3.6.3) was used to perform quality control, read trimming and identification of amplicon sequence variants (ASV's). The S**Error! Bookmark not defined.**ilva reference database (version 138) [49] was used for taxonomic assignment. Raw sequence data are accessible in the sequence read archive (accession number pending). Bacterial ASVs that could not be assigned to a Phylum-level taxonomy were excluded. Samples with <1000 reads were excluded. Prevalence filtering excluded ASVs that were present in only one sample. The Shannon diversity index was used to estimate alpha diversity, based on the number of unique ASVs and their evenness of distribution. Statistical significance for diversity was tested using the Wilcoxon rank sum test. Beta diversity was calculated using the Bray-Curtis divergence on proportional (total sum scaled) data using the vegan package (version2.5-6), with PERMANOVA performed using the *adonis* function (999 permutations). Data analysis was performed through the phyloseq package (version 1.30.0) [50]. Plotting was performed with ggplot2 (version 3.3.2) and ggpubr (version 0.4.0).

Targeted quantitative metabolomics

Samples were lyophilized (3mg) and weighted. The method has been described previously [42]. Finally, 5µL were injected into the LC-MS (XEVO-TQ-XS, Waters®). A Kinetex C18 xb column (1.7µm x 150mm x 2.1mm, temperature 55°C) associated with a gradient of two mobile phases (Phase A:Water + 0.5% formic acid; Phase B: MeOH + 0.5% formic acid) at a flow rate of 0.4mL/min was used.

For each metabolite, a calibration curve was created by calculating the intensity ratio obtained between the metabolite and its internal standard. These calibration curves were then used to determine the concentrations of each metabolite in patient samples.

Radio-Ligand Binding Assay

Cytosolic protein extracts from murine hepatoma Hepa1c1c7 cells (2mg/mL) were incubated for 2 h at room temperature with 2nM [^{3}H]-TCDD in the presence of KYNA (10–1000µM), XANA (10–1000µM), FICZ (100nM; positive control), or vehicle (DMSO; 0.1% V/V; corresponds to specific binding of [^{3}H]-TCDD = 100%). Ligand binding to the cytosolic proteins was determined by the hydroxyapatite binding protocol and scintillation counting as described elsewhere [43]. Specific binding of [^{3}H]-TCDD was determined as a difference between total and non-specific (TCDF; 200nM) reactions. Three independent experiments were performed, and the incubations and measurements were done in triplicates in each experiment (technical replicates). For statistical analysis One-way ANOVA followed by Dunnett's test was performed.

Immunofluorescence detection of the AhR nuclear translocation [51]

LS180 (90,000 cells/well) were grown on poly-D-lysine coated 8-well tissue culture chamber slides (Sarstedt) overnight. The cells were incubated with a vehicle (DMSO; 0.1% V/V), two positive controls (TCDD; model AhR ligand; 10nM and FICZ; endogenous AhR ligand; 10nM), KYNA (100µM), or XANA (100µM) for 90min. After the treatment, the cells were washed with PBS, fixed with 4% (V/V) formaldehyde, permeabilized using 0.1% (V/V) Triton X-100, blocked with 3% (m/V) bovine serum albumin and incubated with Alexa Fluor 488 labelled primary antibody against AhR (sc-133088, Santa Cruz Biotechnology), as described elsewhere [51]. Nuclei were stained with 4′,6-diamino-2-phenylindole (DAPI) and the slides were sealed by coverslips using VectaShield® Antifade Mounting Medium (Vector Laboratories). The AhR nuclear translocation was observed using Oympus Fluoview 1000 confocal system.The experiments were performed in three consecutive cell passages. The level of AhR nuclear translocation was calculated as the proportion of fluorescence intensity of nucleus and fluorescence intensity of cytoplasm (fluorescence of nucleus/fluorescence of cytoplasm) and was expressed as a percentage of intensity of cytoplasm fluorescence. The level of nuclear translocation of AhR was estimated in 80-110 cells for every treatment in

each experiment. For statistical analysis One-way ANOVA followed by Dunnett's test was performed.

AADAT production

Cloning of murine AADAT in *Escherichia coli.* The pMA:muAADAT plasmid carrying the gene encoding murine AADAT (muAADAT) with was synthesized based on *Escherichia coli* codon usage (GeneArt). The DNA fragment coding for muAADAT was then recovered after digestion with *Nhe*I and *Xho*I restriction enzymes and cloned into pStaby 1 vector (DelphiGenetics). The use of pStaby 1 plasmid (**Figure S7B-C**) allows the gene transcription under the control of the phage T7 RNA polymerase promoter (T7 polymerase) and the introduction of a C-terminal six-Histidine tag (His-tag), allowing subsequent purification of muAADAT using affinity chromatography. The resulting final vector pStaby:muAADAT (**Figure S7C**) was transferred into T7 Express Competent *E. coli* (NEB) and transformants were grown at 37°C overnight (ON) in Luria-Bertani medium containing ampicillin (Amp, 100µg/mlL) with shaking at 180rpm. Plasmid DNA was extracted from positive clones and sequenced to confirm their identity.

Expression and purification of the recombinant murine AADAT protein in *E. coli. E. coli* strain expressing muAADAT was cultured at 37°C ON in LB supplemented with Amp 100µg/ml and with shaking. When an optical density (OD 600nm) of 0.8-1.0 was reached, gene expression was induced by the addition of 0.25mM IPTG and the cultures incubated at 16°C ON with stirring at 180rpm (**Figure S7D**). Bacteria were harvested by centrifugation and the cell pellets washed with PBS and resuspended in Binding Buffer (PBS buffer pH 7.4-300mM NaCl supplemented with 0.1% 10X triton and 1X protease inhibitors. Roch). The cells were then sonicated in ice with an amplitude of 40%. The lysate is then centrifuged at 15,000g for 30min at 4°C. The soluble fraction containing AADAT was purified by affinity chromatography. The supernatant were incubated with Ni-NTA agarose resin (R901-15, Invitrogen) at 4°C for 1h then deposited in a BioRad column. The AADAT protein fixed to the resin was washed with PBS buffer, then PBS buffer-20mM imidazole and PBS buffer-40 mM

imidazole. The AADAT protein was eluted with PBS buffer-300mM imidazole (**Figure S7E**). The fractions 2-6 were pooled and dialyzed against PBS, 50% glycerol-300mM NaCl Specta/Port 6. A pre-cast BioRad mini-protean TGX stain free, 4-20% gel was carried out to control the different stages of the purification.

AADAT activity test verification. The AADAT activity test is based on the disappearance of kynurenine which is the substrate of AADAT. A reaction mixture containing 10mM L-kynurenine, 2mM α-oxoglutarate, 40µM PLP (pyridoxal 5′-phosphate) and 0 or 1µL of the purified protein sample prepared in buffer 100 mM potassium phosphate (pH 7.4). Then, the mixture was incubated at 37°C for 15min, and the reaction was stopped by the addition of an equal volume of 30% acetic acid. The supernatant of the reaction mixture, obtained by centrifugation at 3000g for 10min at 4°C, was mixed equally with Ehrlich's solution and incubated 15min at room temperature to have a colorimetric reaction. In parallel, a standard range of kynurenine from 0µM to 1000µM was made under the same conditions. The amount of kynurenine present in the sample was measured with a spectrophotometer at an OD of 492nm and calculated using the standard range (**Figure S7F**). A verification of the production of KYNA and XANA *in vitro* via the action of our enzyme during 15min in the presence of KYNU (1000 µM) was carried out (**Figure S7F**). A dose effect can be observed from the transformation of KYNU into KYNA and XANA.

Statistical analysis

Statistical analysis of human data was performed in the R statistical environment (R version 3.6.2). Plotting was performed with ggplot2 (version 3.3.2). In all statistical analyses, differences with p values <0.05 were considered significant. The p values were corrected using the Benjamini and Hochberg (BH) procedure to control for the false discovery rate. The other data were analyzed using Prism version 8 (Graphpad Software, San Diego, USA). Values are expressed as mean ± Standard error of the mean (SEM). Microbiota-specific analysis is described in the 16S sequencing analysis section. For p value: *: p<0.05, **: p<0.01, ***: p<0.001, ****: p<0.0001.